

# **Perceptual learning in contour detection transfer across changes in contour path and orientation**

Yue Ding<sup>1,2†</sup>, Hongqiao Shi<sup>1,2†</sup>, Shuang Song<sup>1,2</sup>, Yonghui Wang<sup>1,2</sup> and Ya Li<sup>1,2\*</sup>

<sup>1</sup>School of Psychology, Shaanxi Normal University, Xi'an 710062, China

<sup>2</sup>Shaanxi Provincial Key Laboratory of Behavior & Cognitive Neuroscience, School of Psychology,

Shaanxi Normal University, Xi'an 710062, China

† authors contributed equally.

\* Corresponding author.

## **Corresponding author:**

Ya Li

School of Psychology, Shaanxi Normal University

No. 199, Chang'an South Road, Yanta District, Xi'an, China

E-mail: [yali@snnu.edu.cn](mailto:yali@snnu.edu.cn)

## **Abstract**

The integration of local elements into shape contours is critical for target detection and identification in cluttered scenes. Previous studies have shown that observers can learn to use image regularities for contour integration and target identification. However, we still know little about the generalization of perceptual learning in contour integration. Specifically, whether training in contour detection task could transfer to untrained contour type, path or orientation is still unclear. In a series of four experiments, human perceptual learning in contour detection was studied using psychophysical methods. We trained participants to detect contours in cluttered scenes over several days, which resulted in a significant improvement in sensitivity to trained contour type. This improved sensitivity was highly specific to contour type, but transfer across changes in contour path and contour orientation. These results suggest that short-term training improves the ability to integrate specific types of contours by optimizing the ability of the visual system to extract specific image regularities. The differential specificity and generalization across different stimulus features may support the involvement of both low-level and higher-level visual areas in perceptual learning in contour detection. These findings provide further insights into understanding the nature and the brain plasticity mechanism of contour integration learning.

## **Introduction**

Segregating objects from backgrounds and identifying them in cluttered scenes is one of the most fundamental visual abilities for human survival, in which contour integration progress that groups local image elements into global shape is very critical. Although, after long-term evolution and development, human observers are better at detecting collinear contours defined by regularities that typically define coherent contours in natural scenes ([Geisler, 2008](#); [Geisler et al., 2001](#); [Sigman et al., 2001](#); [Simoncelli & Olshausen, 2001](#)) than contours defined by regularities (e.g., elements orthogonal to the contour path) that typically define discontinuities ([Bex et al., 2001](#); [Field et al., 1993](#); [Hess & Field, 1999](#); [Ledgeway et al., 2005](#); [Geisler et al., 2001](#); [Vancleef & Wagemans, 2013](#)). Previous studies have shown that short-term perceptual training in adulthood could also

improve observers' ability to detect contours defined by regularities that typically signify continuities or discontinuities (Schwarzkopf & Kourtzi, 2008; Schwarzkopf & Kourtzi, 2009; Zhang & Kourtzi, 2010). However, we know little about the exact nature of perceptual learning of contour integration. A lot of perceptual learning studies revealed that the learning of basic simple stimulus features such as contrast, orientation, etc., is specific to the trained retinal location and feature (Ball & Sekuler, 1982, 1987; Liu, 1999; Fiorentini & Berardi, 1981; Schoups et al., 1995; Yu et al., 2004). As perceptual learning of relatively complex stimuli, over which features, and to what extent, contour integration learning exhibits specificity or transferability is still not well understood.

In this study, we examined the specificity and transferability of contour integration learning over contour type (i.e., the local orientation alignment of contour elements), global contour path, and global contour orientation through four experiments using the contour detection task. We tested participants' performance in detecting contours, with different contour types, contour paths, or contour orientations, before and after training on orthogonal contours (i.e., elements orthogonal to the contour path). We found that the learning effect was specific to contour type but partially transferable over contour path and contour orientation, indicating both the low-level and higher-level visual areas were engaged in the learning of contour integration and detection. These findings advance our understanding of the nature and brain plasticity mechanisms of contour integration learning.

## **Materials and Methods**

### **Experiment 1**

#### Participants

Twenty native participants (eight males; age:  $20.50 \pm 2.19$  years) with normal or corrected-to-normal vision took part in this experiment. They were naive to the purpose of the study and had no previous experience with contour integration experiments. Ten subjects participated in Experiment

1A (three males; age:  $20.90 \pm 1.79$  years), and ten subjects participated in Experiment 1B (four males; age:  $20.10 \pm 2.56$  years). All participants gave written informed consent before the experiment and were paid for their participation. This project was approved by the local ethics committee.

## Apparatus and stimuli

All procedures were programmed using PsychToolbox-3 (Brainard, 1997; Kleiner et al., 2007) for MATLAB (MathWorks, Natick, MA). Stimuli were generated with GERT (Grouping Elements Rendering Toolbox; Demeyer & Machilsen, 2012) called from MATLAB and presented on a 27-in IPS monitor with a resolution of  $2560 \times 1440$  and a refresh rate of 100Hz. Subjects viewed the stimuli at a distance of 67 cm in a darkened room, and a chin-and-head rest was used to stabilize their heads.

The stimuli for the contour detection task were Gabor fields (radius:  $4.1^\circ$  of visual angle) comprising 170-190 Gabor elements (Gaussian windowed cosinusoidal gratings, peak spatial frequency: 8.3 cycle/deg, envelope  $\sigma$ :  $0.08^\circ$ , contrast: 100%) and presented on an equiluminant gray background (mean luminance: 43 cd/m<sup>2</sup>). The minimal distance between any element and its nearest neighbor was  $0.42^\circ$ , which ensured that there were no local density cues in any Gabor fields.

In contour stimuli, there were four contours, that were composed of 28 Gabor elements, embedded in a background of randomly positioned and oriented Gabor elements (see Fig. 1). The contours were defined by elements that could be aligned along the invisible contour path (collinear contours) or perpendicular to the path (orthogonal contours). The mean inter-element separation of contour elements was  $0.64^\circ$  and the position jitter (the relative position of the elements jittered along the contour or perpendicular to the contour) was  $\pm 0.13^\circ$ .

In our study, there were two types of global contour paths: straight path and curved path. For the straight path (see Fig. 1), the global orientation of the four parallel lines was randomly chosen between  $20^\circ$ - $80^\circ$  and  $110^\circ$ - $160^\circ$  in increments of  $5^\circ$  (except  $45^\circ$  and  $135^\circ$ ). The mean distance between the four target contours was  $1.88^\circ$  with a  $0.06^\circ$  jitter. For the curved path (see Fig. 1), four semicircular curves symmetrical about the center were arranged opposite to each other. The mean curvature of these four paths was  $14.4^\circ$ . The global orientation of the symmetry axis was determined

in the same way used in the straight path conditions. The mean distance between the four target contours was  $1.88^\circ$  and has the same jitter as the straight path. Furthermore, in this study, the alignment of local contour elements relative to their mean orientation was jittered by an angle range. In test sessions, the orientation jitter of local contour elements was either  $\pm 0^\circ$ ,  $\pm 10^\circ$ ,  $\pm 20^\circ$ ,  $\pm 30^\circ$ , or  $\pm 45^\circ$ . In training sessions, the jitter depended on the participant's performance and was determined by an adaptive staircase method (see the procedure for details).

Corresponding to contour stimuli, we also generated random stimuli. That is, for every stimulus in each condition (collinear-straight contours, collinear-curved contours, orthogonal-straight contours, orthogonal-curved contours), we created a random stimulus by shuffling the local orientations of all the elements in the Gabor field.

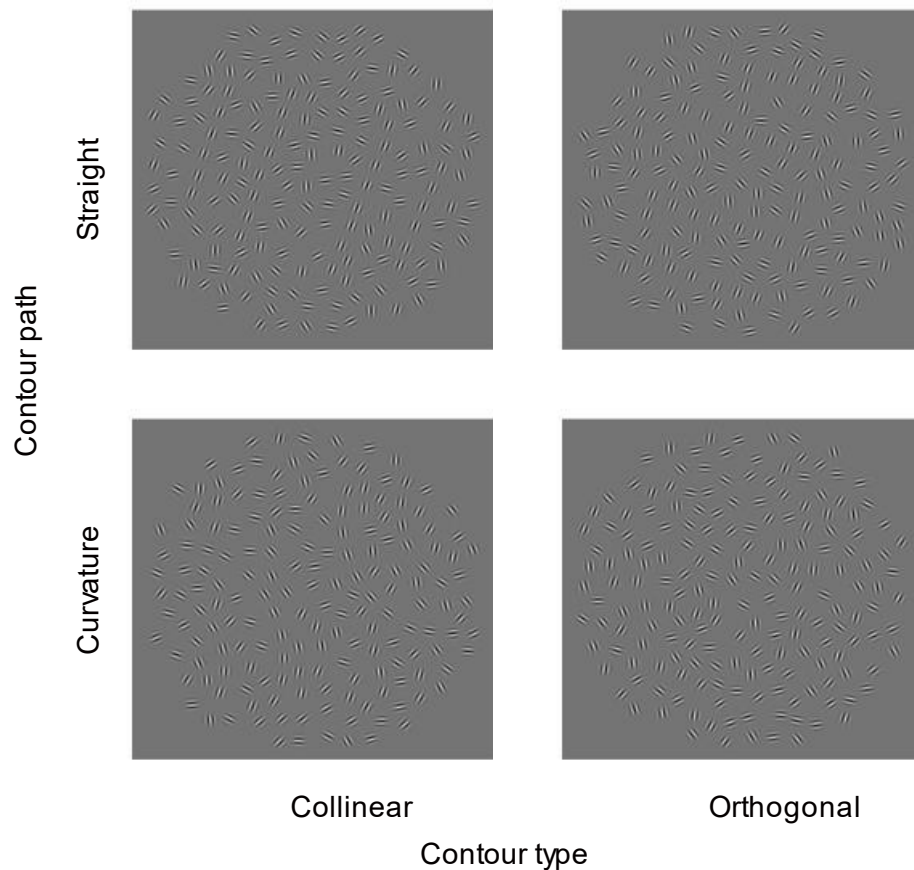


**Figure 1.** Stimuli in experiments 1a and 1b. Examples in each row show the same contour path (straight or curved). Stimuli on the left and right are collinear contours and orthogonal contours, respectively.

## Experimental design and statistical analysis

All experiments (experiment 1a and experiment 1b) consist of four phases: (1) pretest, (2) 5-day training, (3) post-test I; and (4) posttest II. Posttest I and posttest II phases were separated for several weeks in order to assess the stability of training effect.

### *Task*

In both test and training sessions, participants performed a two-interval forced-choice (2IFC) contour detection task. As shown in Fig. 2, each trial started with a central fixation of a red dot presented for 500-ms. Two Gabor field stimuli separated by a 500-ms fixation interval were sequentially presented for 300-ms in random order. One of them contained the target contours and the other was a random stimulus. Participants were asked to indicate which interval contained the contours by pressing one of two buttons within 3000-ms after the second stimulus vanished. Moreover, they were required to maintain fixation during the whole experiment and respond as accurately and quickly as possible.

### *Staircase procedure*

To quantify participants' ability of contour detection on every training day, we used an adaptive staircase method (3-up-1-down, step size of  $1^\circ$ ), which converged at a performance level of 79.4% accuracy. Each staircase consisted of 7 preliminary reversals and 8 experimental reversals. The staircase block ended when there were 15 reversals or participants completed 100 trials. The geometric mean of the experimental reversals was taken as the threshold for each staircase block.

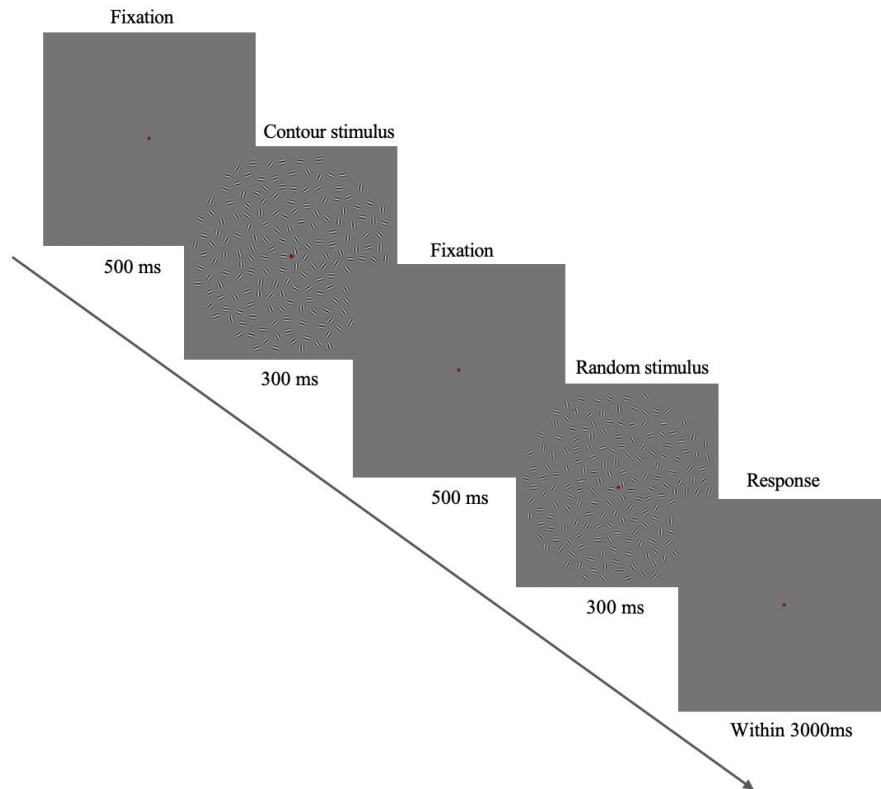


**Figure 2.** Experimental procedures. An example trial of the contour detection task in the test and training phase.

### *Test sessions (pretest, posttest, posttest II)*

These test sessions consisted of four experimental conditions (2 contour types  $\times$  2 contour paths) with five orientation jitters ( $0^\circ$ ,  $10^\circ$ ,  $20^\circ$ ,  $30^\circ$ ,  $45^\circ$ ) to assess the effect of learning and transfer. Participants completed 800 trials (40 trials per jitter level per condition) in each session and had a rest every 40 trials. All stimuli were presented randomly and no feedback was given in these sessions.

We quantified the ability of participants to detect contours embedded in a cluttered pattern by two measures: accuracy at  $0^\circ$  jitter, and the orientation jitter at 70% correct performance (threshold) fitting a cumulative Gaussian function.

On the first day, all participants were given three brief familiarization runs before commencing the pretest session. All runs had auditory feedback on incorrect responses. In the first run, participants only practiced  $0^\circ$  jitter contours (4 trials per condition) which were presented for 1000-ms. In the second run, participants also practiced  $0^\circ$  jitter contours but stimuli presentation time was shortened to 300-ms (same as the formal experiment). In the third run, participants practiced all jitter contours for 80 trials, and the procedure was as same as the pretest session except for auditory feedback.

### *Training sessions*

The task and stimuli in training sessions were identical to those used in test sessions. Participants were trained on a contour detection task with different contour conditions for 5 days. One group of participants was trained on orthogonal-straight contours (Experiment 1a,  $n=10$ ), and the other was trained on orthogonal-curved contours (Experiment 1b,  $n=10$ ). During the whole training session, auditory feedback was given on incorrect trials.

The detection thresholds were estimated by an adaptive staircase method (3-up-1-down, step size of  $1^\circ$ , 15 reversals). The training session on each day included 15 blocks. For the first block of the first day, the starting orientation jitter was  $0^\circ$ . Then the start jitter value in subsequent staircase blocks followed the preceding block. The threshold in each block was determined by the mean orientation jitter of the last eight reversals, and the threshold of the day was calculated by averaging these 15 blocks. Furthermore, for the next day, the orientation jitter of the first block was the one used in the last block the day before.

### *Data analysis*

To validate the training effect, we used a paired-samples t-test to compare the detection thresholds between the first and last sessions of the training phase. To examine the effect of training on detection performance in the test phases and to inspect whether the learning effect could transfer to untrained contour conditions, we performed one-sample t-tests on four conditions' (2 contour type  $\times$  2 contour path) mean improvement (MI, posttest-pretest) of threshold (two-tailed, compared with 0). We applied false discovery rate (FDR) method to correct  $p$  values for multiple comparisons across conditions. Furthermore, we conducted a two-way (contour type  $\times$  contour path) repeated-measures ANOVA on the MI of threshold to compare the improvement between different conditions.

Consistent with previous research, we used a transfer index (TI), which is a quotient of the improvement on the threshold at the transfer condition divided by the improvement on the trained condition, to quantify the transfer effect and compared it among different experiments. As is known that  $TI = 0$  indicates complete learning specificity. Instead,  $TI = 1$  indicates complete learning transfer.

## Experiment 2

### Participants

Twenty-one participants (seven males; age:  $20.43 \pm 1.97$  years) with normal or corrected-to-normal vision took part in this study. They were naive to the purpose of the study and had no previous experience with contour integration experiments. Ten subjects participated in experiment 2a (three males; age:  $19.90 \pm 1.97$  years), and eleven subjects participated in experiment 2b (four males; age:  $20.91 \pm 1.30$  years). All participants gave written informed consent before the experiment and received a monetary reward. This study was approved by the local ethics committee.

### Apparatus and stimuli

The stimuli in Experiment 2 were identical to those in Experiment 1, except for the following three aspects: 1) adding a contour type (see Fig. 3) that the local contour elements were aligned at an acute angle ( $30^\circ$ ) to the contour path (acute contours); 2) decreasing mean inter-element separation of contour elements to  $0.58^\circ$ ; 3) increasing the number of curved contour elements to 34. The purpose of the last two points was to control the task difficulty across different contour conditions (especially for orthogonal-curved, orthogonal-straight, acute-curved, and acute-straight).

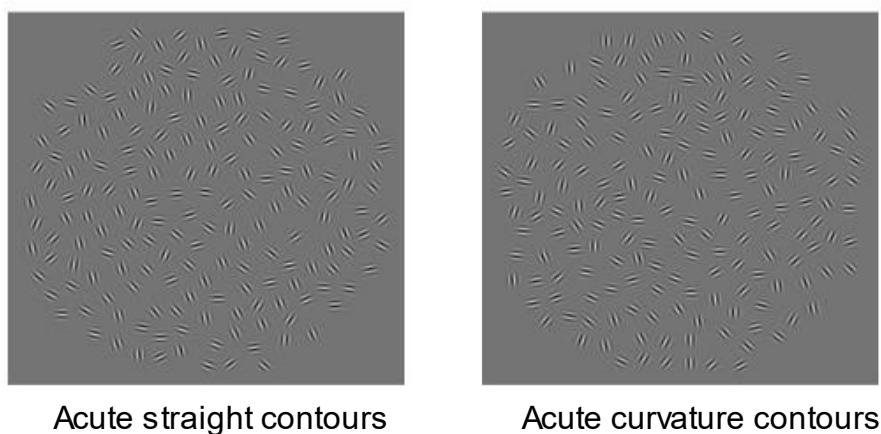


**Figure 3.** Acute contour stimuli in experiments 2. Examples of acute contour stimuli in which contour paths are straight (left) and curved (right).

## Experimental design and statistical analysis

### *Procedure*

The general procedure in Experiment 2 was mostly identical to that in Experiment 1, except that there were seven sessions of training in the current experiment. Furthermore, because of adding another contour condition, we increased the trial number to 1200 and divided all test sessions (including pretest, posttest, and second posttest) into two days to avoid the fatigue effect.

### *Data analysis*

Mostly the same as Experiment 1, a paired-samples t-test was performed in training sessions to examine the training effect. One-sample t-test for six contour conditions (3 contour types  $\times$  2 contour paths) on MI of the threshold was performed to investigate the effect of training on detection performance in the test phases and inspect whether the learning effect could transfer to untrained contour conditions (two-tailed, compared with 0). Multiple comparisons were corrected by using false discovery rate (FDR) method. We also conducted a two-way (contour type  $\times$  contour path) repeated-measures ANOVA on the MI of threshold to compare the improvement between different conditions and calculated TI (based on MI of the threshold) to quantify the transfer effect and compare it across experiments.

## Experiment 3

### Participants

A total of twenty subjects (five males; age:  $18.39 \pm 3.95$  years) with normal or corrected-to-normal vision participated in Experiment 3. They were not told the purpose of the study and had no previous experience with contour integration experiments. Ten subjects participated in Experiment 3a (two males; age:  $18.60 \pm 1.80$  years), and ten subjects participated in Experiment 3b (three males; age:  $19.80 \pm 1.75$  years). All participants gave written informed consent before the experiment and received a monetary reward. This study was approved by the local ethics committee.

## Apparatus and stimuli

The contour stimuli we used in Experiment 3 were only orthogonal contours oriented around  $45^\circ$  and  $135^\circ$  with a range of  $\pm 15^\circ$  (see Fig. 4). Apart from this, other aspects were the same as those in Experiment 2.

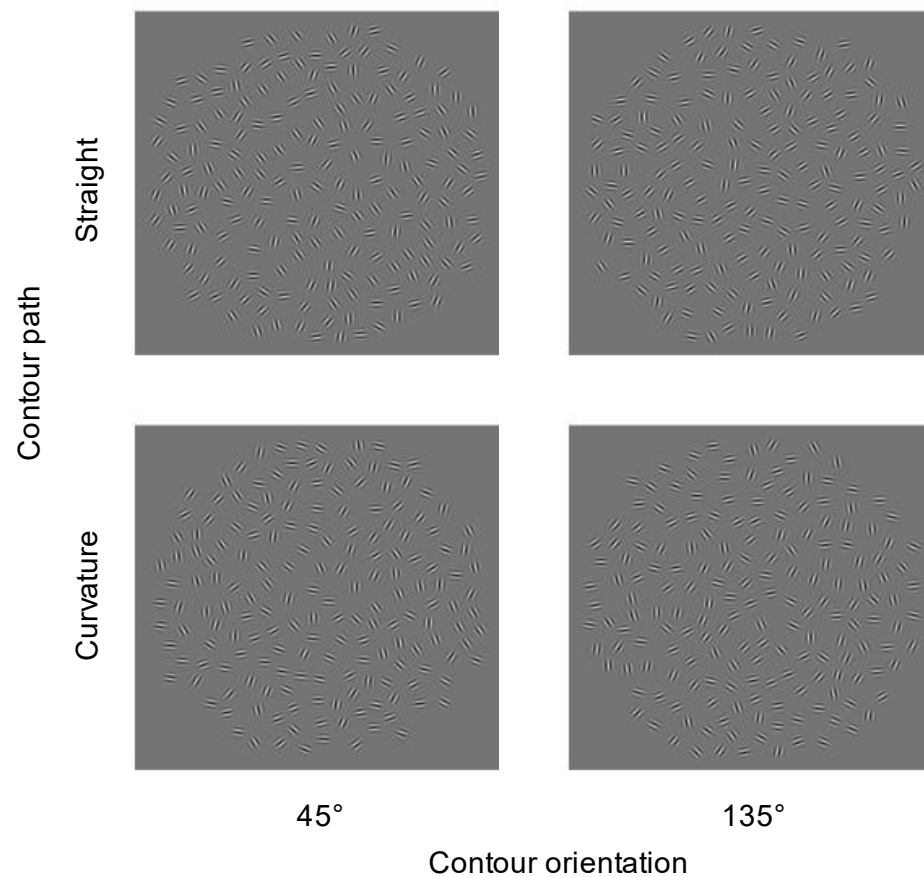


**Figure 4.** Stimuli in experiments 3a and 3b. Examples in each row show the same contour path (straight or curved). Stimuli on the left and right are orthogonal contours oriented at  $45^\circ$  and  $135^\circ$ , respectively.

## Experimental design and statistical analysis

### *Task*

As with Experiment 1 and Experiment 2, there were four phases in Experiment 3: (1) pretest (1 day), (2) training (7 days), (3) post-test I (1 day); and (4) posttest II (1 day). To assess the stability of training effect, the same participants performed posttest II several weeks after they completed posttest I. Similarly, the subjects also performed the contour detection task in this experiment.

### *Test sessions (pretest, posttest, posttest II)*

All test sessions comprised the same four experimental conditions (2 contour orientations  $\times$  2 contour paths). For each experiment condition, we set five levels of local contour elements' orientation jitter (0°, 10°, 20°, 30°, 45°) to assess the effect of learning and transfer. Participants completed 800 trials (40 trials per jitter level per condition) in each session and had a rest every 40 trials. All stimuli were presented randomly and no feedback was given in these sessions.

### *Training sessions*

The task and procedure during the training sessions were the same as those during the test sessions. During 7-days training sessions, participants were presented with one of four experimental conditions only and received auditory feedback on incorrect responses. Subjects in Experiment 3a and Experiment 3b were trained on straight contours and curved contours respectively. To maintain balance, one-half of the participants were trained to detect contours oriented at 45°, and the other half were trained to detect contours oriented at 135°, in both Experiment 3a and Experiment 3b.

### *Data analysis*

Similarly, we performed a paired-samples t-test on training sessions to examine the training effect. Furthermore, one-sample t-tests for four contour conditions (2 contour orientations  $\times$  2 contour paths) on MI of the threshold were performed to investigate the effect of training and transfer of the learning effect (two-tailed, compared with 0). The *p*-values of multiple comparisons across conditions were corrected by using false discovery rate (FDR) method. We also conducted a two-way (contour path  $\times$  contour orientation) repeated-measures ANOVA on the MI of threshold to compare the improvement between different conditions. To quantify the transfer effect and compare transfer patterns, we calculated TI (based on the MI of threshold) and performed a one-sample t-test on it (two-tailed, compared with 0 and 1).

## **Experiment 4**

### Participants

A total of twenty participants (seven males; age:  $19.25 \pm 1.12$  years) with normal or corrected-to-normal vision took part in Experiment 4. They were naive to the purpose of the study and had no

previous experience with contour integration experiments. Ten subjects participated in experiment 4a (four males; age:  $19.30 \pm 0.82$  years), and ten subjects participated in experiment 4b (three males; age:  $19.20 \pm 1.40$  years). All participants gave written informed consent before the experiment and received a monetary reward. This study was approved by the local ethics committee.

## Apparatus and stimuli

To test training-dependent changes for orthogonal contours, we introduced acute contours (see Fig. 5) for four experimental conditions of Experiment 3 in this experiment. That is, for each condition of four stimulus conditions ( $2$  contour orientations  $\times 2$  contour paths), we generated contour stimuli in which local contour elements were aligned orthogonally to the path and contour stimuli in which local contour elements were aligned at an acute angle ( $30^\circ$ ) to the path.

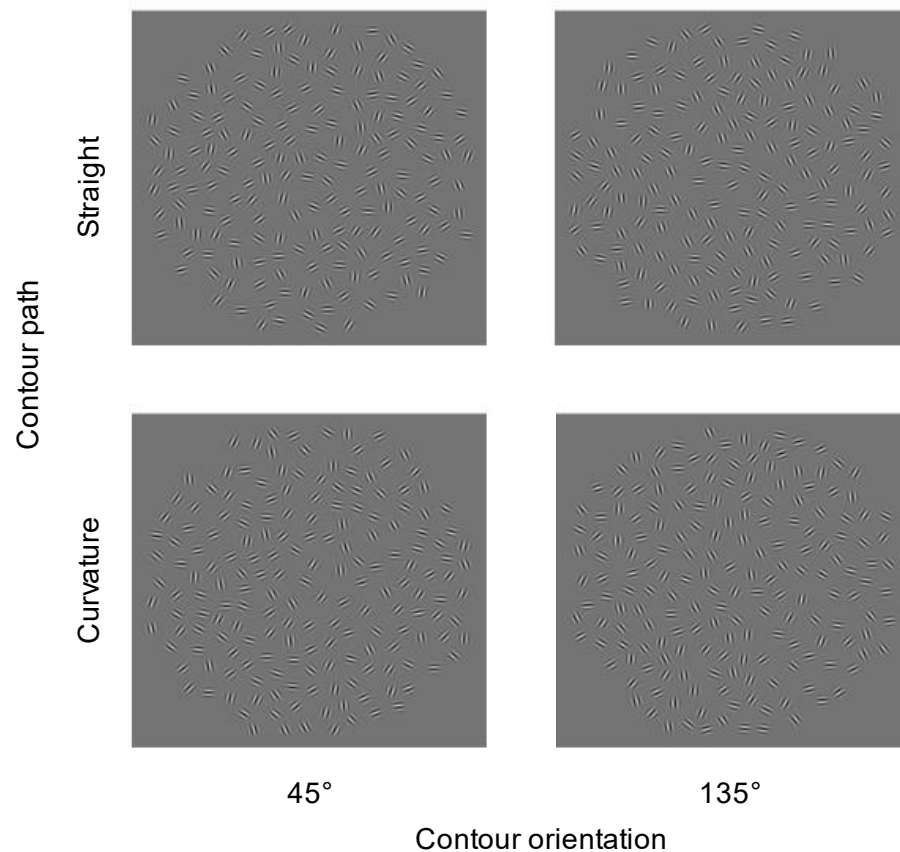


**Figure 5.** Acute contour stimuli in experiments 4. Examples in each row contain the same contour path (straight or curved). Stimuli on the left and right are acute contours oriented at  $45^\circ$  and  $135^\circ$ , respectively.

## Experimental design and statistical analysis

### *Procedure*

In Experiment 4, each test session comprised eight experimental conditions (3 contour types  $\times$  2 contour orientations  $\times$  2 contour paths), due to the introduction of acute contours. We had to increase the trial number of each test session to 1600 and divided all test sessions (including pretest, posttest, and second posttest) into two days (800 trials per day) to avoid the fatigue effect. Except for this, there was no difference between the procedure of Experiment 4 and that of Experiment 3.

### *Data analysis*

As we did in the above experiments, we performed similar paired-samples t-tests and one-sample t-tests on the threshold to examine the training effect and the transfer of learning. Consistent with our experimental design, we conducted a three-way (contour type  $\times$  contour path  $\times$  contour orientation) repeated-measures ANOVA on the MI of threshold to compare the improvement between different conditions.

# Result

## Experiment 1a

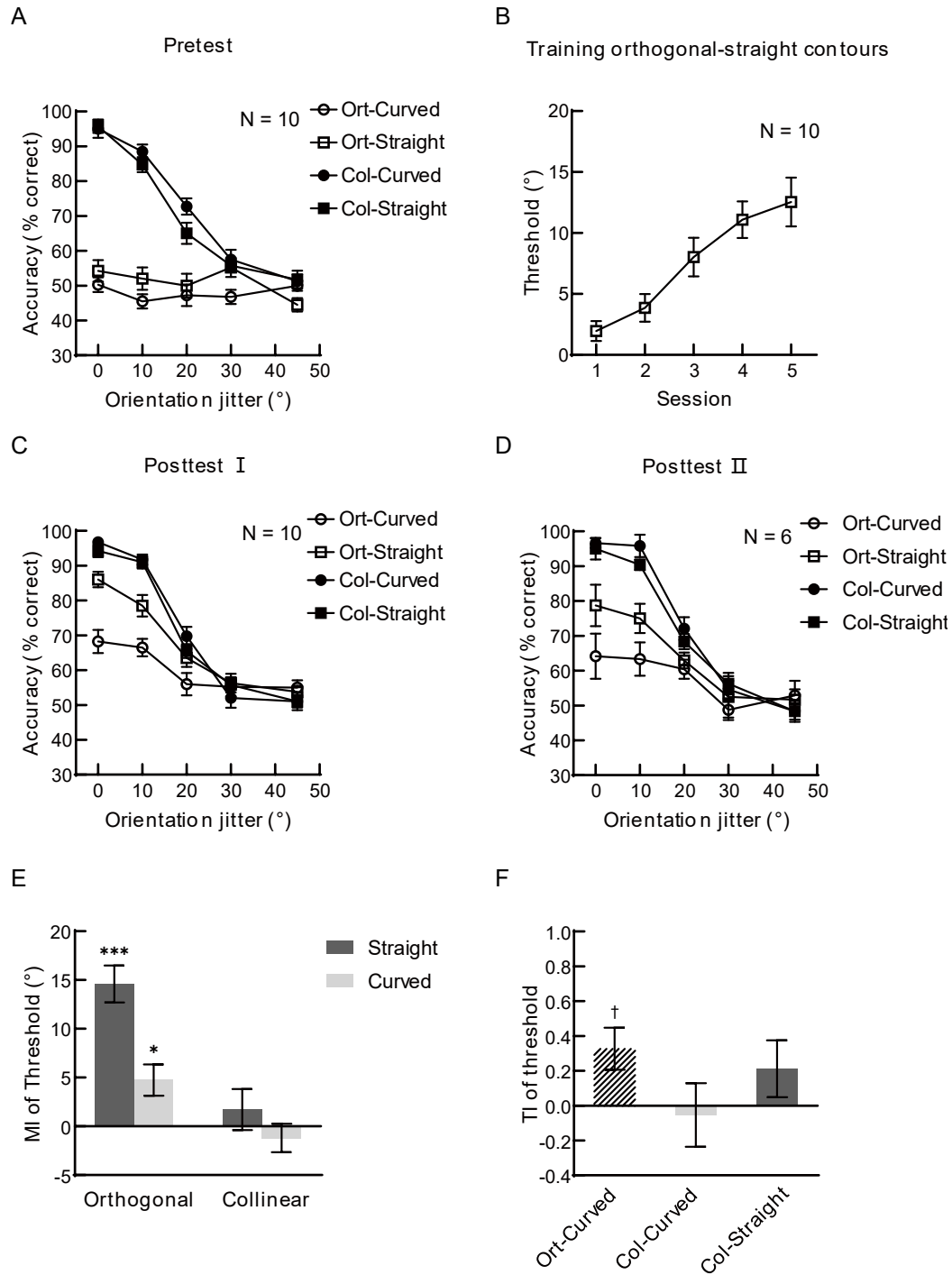


**Figure 6.** Training on Orthogonal-Straight Contours in Experiment 1a. (A) Psychometric curves (averaged across participants) for contour detection performance (percent correct) plotted as a function of local orientation jitter before training on orthogonal-straight contours. (B) Detection

performance for each training session. (C) Psychometric curves for performance (percent correct) plotted as a function of local orientation jitter after training. (D) Psychometric curves for performance (percent correct) tested 3-16 weeks after training. (E) MI of detection thresholds for trained and untrained conditions after training on orthogonal-straight contours. (F) TI of detection thresholds for untrained conditions. Asterisks indicate significant difference with 0. Error bars represent standard error of the mean across participants.

*Improved performance in detecting orthogonal contour both for trained and untrained path*

In Experiment 1a, we trained participants on the detection of orthogonal-straight contours with auditory feedback. After training, participants' sensitivity to detecting orthogonal-straight contour was improved across training sessions (Figure.6B). The threshold measurement of the last training session was significantly higher than the measurement of the first training session ( $t_{(9)} = 5.41, p < 0.001$ , Cohen's  $d = 1.71$ ).

Figure. 6A and Figure. 6C show participants' performance in the pretest session and posttest I session, respectively. To examine the effect of training on detection performance and to inspect whether the learning effect can transfer to other contour conditions, we performed one-sample t-tests (two-tailed, compared with 0) on four conditions' (2 contour types  $\times$  2 contour paths) mean improvement (MI, posttest-pretest) of threshold (Figure. 6E). For training (orthogonal-straight) condition, we observed significant improvement of threshold ( $t_{(9)} = 7.73, p < 0.001$ , Cohen's  $d = 2.44$ ; FDR-corrected), indicating a significant learning effect. Furthermore, we also observed significant improvement in detecting the untrained orthogonal-curved condition ( $t_{(9)} = 2.90, p = 0.033$ , Cohen's  $d = 0.93$ ; FDR-corrected), which shared the same contour type (orthogonal) with training condition,. However, there was no significant improvement for the other two untrained conditions: collinear-straight contours ( $t_{(9)} = 0.82, p = 0.434$ , Cohen's  $d = 0.26$ ; FDR-corrected) and collinear-curved contours ( $t_{(9)} = -0.82, p = 0.434$ , Cohen's  $d = -0.26$ ; FDR-corrected). The results showed that the learning effect for the training condition could transfer to the untrained condition which contained the same contour type as the trained one but failed to do it when the untrained conditions contained different contour type, and may suggest the learning of image regularity (contour type) after contour-detection training.

In addition, there was no significant difference in the performance of participants ( $n=6$ ) between the posttest immediately after training and the second posttest 3-16 weeks after training

(threshold:  $t_{(5)} = 0.63$ ,  $p = 0.558$ , Cohen's  $d = 0.26$ ), which indicated that the learning effect for orthogonal-straight contours could be maintained for a prolonged period (Figure. 6C vs. Figure. 6D).

*Partial transfer of learning effect across contour paths when training on the straight path*

A two-way (contour type  $\times$  contour path) repeated-measures ANOVA on the MI of threshold showed a significant main effects of contour type ( $F_{(1,9)} = 15.79$ ,  $p = 0.003$ ,  $\eta_p^2 = 0.64$ ) and contour path ( $F_{(1,9)} = 23.28$ ,  $p < 0.001$ ,  $\eta_p^2 = 0.72$ ), indicating more training-induced improvement for the trained type and path versus untrained type and path. The interaction between contour type and contour path showed a trend of significance ( $F_{(1,9)} = 4.92$ ,  $p = 0.054$ ,  $\eta_p^2 = 0.35$ ). Further simple effect analysis revealed significantly larger MI of straight path than curved path ( $t_{(9)} = 4.77$ ,  $p = 0.001$ , Cohen's  $d = 2.27$ ) only for orthogonal contours (Figure. 6E).

Furthermore, we calculated the TI of threshold to quantify the transfer effect (Fig. 6F). In the current experiment, TI of the transfer condition (orthogonal-curved contours) showed a trend of significantly higher than 0 ( $t_{(9)} = 2.71$ ,  $p = 0.073$ , Cohen's  $d = 0.86$ ; FDR-corrected), but significantly lower than 1 ( $t_{(9)} = -5.58$ ,  $p < 0.001$ , Cohen's  $d = -1.77$ ; FDR-corrected), suggesting a partial transfer of contour-detection learning between contour paths. However, TI for other untrained conditions (contours with untrained type) showed no significant difference with 0 (collinear-curved contours:  $t_{(6)} = -0.29$ ,  $p = 0.777$ , Cohen's  $d = -0.09$ ; collinear-straight contours:  $t_{(6)} = 1.3$ ,  $p = 0.339$ , Cohen's  $d = 0.41$ ; FDR-corrected:).

## Experiment 1b

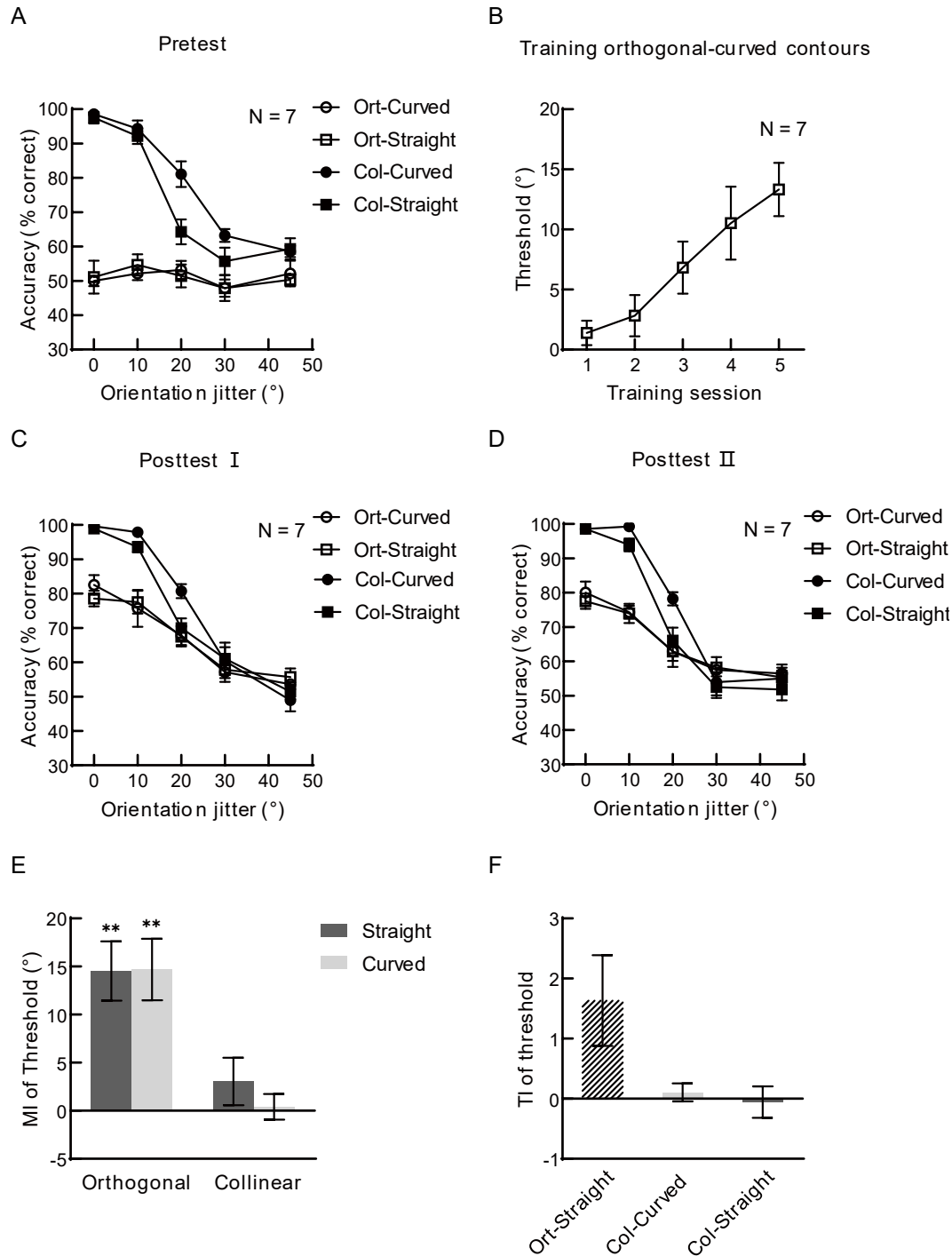


**Figure 7.** Training on Orthogonal-Curved Contours in Experiment 1b. (A) Psychometric curves (averaged across participants) for contour detection performance (percent correct) plotted as a function of local orientation jitter before training on orthogonal-curved contours. (B) Detection performance for each training session. (C) Psychometric curves for performance (percent correct) plotted as a function of local orientation jitter after training. (D) Psychometric curves for performance (percent correct) tested 3-16 weeks after training. (E) MI of detection thresholds for

trained and untrained conditions after training on orthogonal-curved contours. (F) TI of detection thresholds for untrained conditions. Asterisks indicate significant difference with 0. Error bars represent standard error of the mean across participants.

*Improved performance in detecting orthogonal contour both for trained and untrained path*

In Experiment 1b, we trained participants to detect orthogonal-curved contours. After training, three of ten participants' detection accuracy at 0° jitter for orthogonal-curved contours in posttest I did not reach 70% correct. The small number of outlier participants could not support conclusive analysis, and therefore, we excluded the data from these participants. Figure 7A and Figure 7C show participants' detection performance before and after training respectively. During the training phase, the threshold measurement of the last training session was significantly higher than the measurement of the first training session ( $t_{(6)} = 6.16, p < 0.001$ , Cohen's  $d = 2.33$ ; Figure 7B).

As in Experiment 1a, we conducted one-sample t-tests (two-tailed, compared with 0) on MI of threshold, to elucidate the learning effect on training condition and the transfer on untrained conditions (Figure 7E). We observed significant learning effect for trained orthogonal-curved contours ( $t_{(6)} = 4.60, p = 0.007$ , Cohen's  $d = 1.74$ ; FDR-corrected). Furthermore, again, the performance for untrained orthogonal-straight contours, which shared the same contour type with training condition, were also significantly improved ( $t_{(6)} = 4.72, p = 0.007$ , Cohen's  $d = 1.78$ ; FDR-corrected). However, we found no significant improvements on collinear-curved contours ( $t_{(6)} = 0.31, p = 0.769$ , Cohen's  $d = 0.12$ ; FDR-corrected) and collinear-straight contours ( $t_{(6)} = 1.24, p = 0.350$ , Cohen's  $d = 0.47$ ; FDR-corrected), which was identical to our findings in Experiment 1a. The learning transfer from trained condition to the untrained transfer condition with untrained contour path but trained contour type may indicate that participants learned the image statistic regularity (contour type) during contour-detection training.

Furthermore, we observed no significant difference in performance on orthogonal-curved contours between the posttest I and the posttest II (threshold:  $t_{(6)} = 0.79, p = 0.460$ , Cohen's  $d = 0.30$ ), indicating that learning effect for training contours lasted for a prolonged period (Figure 7C vs. Figure 7D).

*Complete transfer of learning effect across contour paths when training on the curved path*

We entered the MI of threshold into a two-way (contour type  $\times$  contour path) repeated-measures ANOVA (Figure. 7E). The ANOVA on threshold showed a significant main effect of

contour type ( $F_{(1,6)} = 30.17, p = 0.002, \eta_p^2 = 0.83$ ), indicating more training-induced improvement for the trained versus untrained type. Neither the main effect of contour path ( $F_{(1,6)} = 0.28, p = 0.614, \eta_p^2 = 0.04$ ) nor the interaction effect ( $F_{(1,6)} = 0.33, p = 0.587, \eta_p^2 = 0.05$ ) reached the significance level, indicating no difference in improvement between contour paths.

We further calculated the TI of thresholds for untrained conditions to quantify the transfer of training effect (Figure 7F). One-sample t-test revealed no significant difference between TI for orthogonal-straight condition (contours with trained contour type but untrained contour path) and 1 ( $t_{(6)} = 0.84, p = 0.435$ , Cohen's  $d = 0.32$ ; FDR-corrected). Consistent with the results of our one-sample t-tests on MI, TI for other untrained conditions (contours with untrained type) showed no significant difference with 0 (collinear-curved contours:  $t_{(6)} = 0.70, p = 0.762$ , Cohen's  $d = 0.27$ ; collinear-straight contours:  $t_{(6)} = -0.22, p = 0.835$ , Cohen's  $d = -0.08$ ; FDR-corrected). These results show a complete transfer of learning effect between contour paths but no transfer of learning effect between contour types, which were not exactly the same as our findings in Experiment 1a.

#### *The effects of training conditions on the degree of learning transfer*

Interestingly, in Experiment 1b (training on orthogonal-curved contours), we observed complete learning transfer between contour paths, rather than partial transfer as in Experiment 1a (training on orthogonal-straight contours). To compare the transfer effects between different training conditions, we conducted an independent-sample t-test on TI for untrained transfer conditions (contours with trained type but untrained path) from Experiment 1a and Experiment 1b. We observed a trend of significant difference between the two training conditions ( $t_{(15)} = 2.12, p = 0.051$ , Cohen's  $d = 1.045$ ). Furthermore, a mixed-design ANOVA on the MI of thresholds with contour type (collinear and orthogonal) and contour path (straight and curved) as within-subject factors and experiment (Experiment 1a and Experiment 1b) as a between-subject factor showed that the three-factor interaction ( $F_{(1,15)} = 0.57, p = 0.462, \eta_p^2 = 0.04$ ), the interaction between experiment and contour type ( $F_{(1,15)} = 1.01, p = 0.330, \eta_p^2 = 0.06$ ) was not significant. The main effects of experiment ( $F_{(1,15)} = 3.57, p = 0.078, \eta_p^2 = 0.19$ ) and path ( $F_{(1,15)} = 4.25, p = 0.057, \eta_p^2 = 0.22$ ) and the interaction between contour type and contour path ( $F_{(1,15)} = 3.12, p = 0.098, \eta_p^2 = 0.17$ ) were marginally significant. The main effect of contour type ( $F_{(1,15)} = 41.72, p < 0.001, \eta_p^2 = 0.74$ ) and the interaction between experiment and contour path ( $F_{(1,15)} = 9.32, p = 0.008, \eta_p^2 = 0.38$ ) were significant. Simple

analysis revealed that, for the untrained contour path, the performance improvement in Experiment 1b was significantly higher than that in Experiment 1a ( $t_{(32)} = 2.75, p = 0.010$ , Cohen's  $d = 0.96$ ). In contrast, there was no significant difference between performance improvement in Experiment 1a and Experiment 1b for the trained contour path ( $t_{(32)} = -0.19, p = 0.852$ , Cohen's  $d = -0.07$ ). These results indicated that the transfer effect between paths was larger when training on curved contours than training on straight contours in this experiment.

We further compared the detection thresholds for training conditions on the fourth day and the fifth day during the training phase in the two experiments, respectively. We observed significantly higher thresholds on the fifth day than on the fourth day in Experiment 1b ( $t_{(6)} = 2.61, p = 0.040$ , Cohen's  $d = 0.99$ ), but no significant difference in performance between the last two days in Experiment 1a ( $t_{(9)} = 1.40, p = 0.195$ , Cohen's  $d = 0.44$ ), which meant that the training in the two experiments might be at different levels. To control the degree of training under different training conditions, we increased the number of sessions in the training phase to 7 in subsequent experiments.

## Experiment 2a

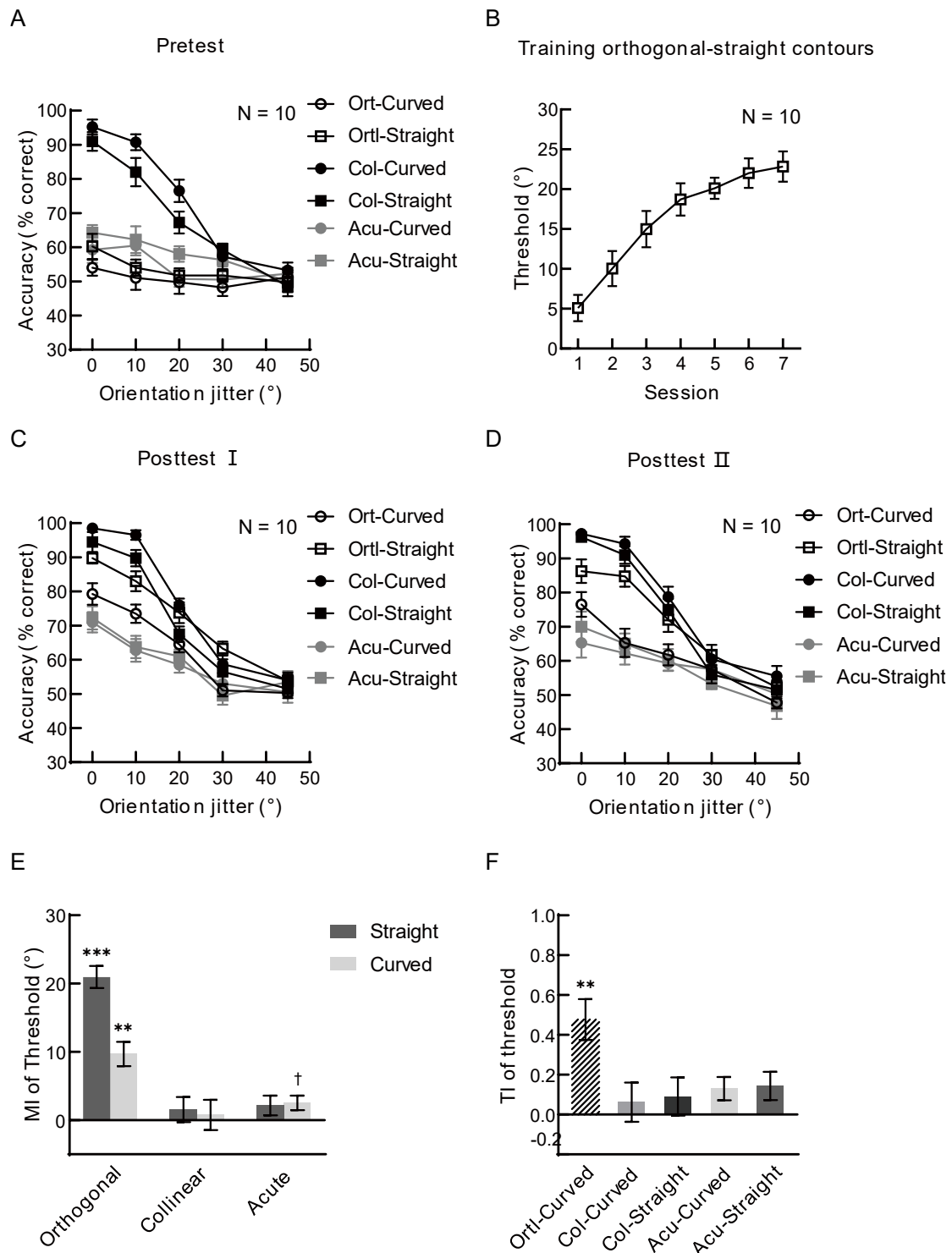


**Figure 8.** Training on Orthogonal-Straight Contours in Experiment 2a. (A) Psychometric curves (averaged across participants) for contour detection performance (percent correct) plotted as a function of local orientation jitter before training on orthogonal-straight contours. (B) Detection performance for each training session. (C) Psychometric curves for performance (percent correct) plotted as a function of local orientation jitter after training. (D) Psychometric curves for

performance (percent correct) tested 3-16 weeks after training. (E) MI of detection thresholds for all conditions after training on orthogonal-straight contours. (F) TI of detection thresholds for untrained conditions. Asterisks indicate significant difference with 0. Error bars represent standard error of the mean across participants.

*Improved performance in detecting orthogonal contours both for trained and untrained paths*

Consistent with previous studies (Schwarzkopf & Kourtzi, 2008; Schwarzkopf & Kourtzi, 2009), our measurement showed that participants' performance in detecting collinear contours was higher than in detecting orthogonal or acute contours before training (Figure 8A). Compared to the first training session, participants' detection threshold for orthogonal-straight contours in the last training session was significantly higher ( $t_{(9)} = 10.46$ ,  $p < 0.001$ , Cohen's  $d = 3.31$ ). Moreover, there was no significant difference between thresholds in the last two training sessions ( $t_{(9)} = 1.30$ ,  $p = 0.225$ , Cohen's  $d = 0.41$ ), indicating that the training for orthogonal-straight contours had reached the asymptotic level.

Similar to Experiment 1, we conducted one-sample t-tests (two-tailed, compared with 0) on six conditions' (3 contour types  $\times$  2 contour paths) MI of threshold after training (Figure 8E), to examine the effect of training on detection performance and inspect the transfer of learning. We observed significantly improved performance for trained orthogonal-straight contours ( $t_{(9)} = 12.90$ ,  $p < 0.001$ , Cohen's  $d = 4.08$ ; FDR-corrected) and untrained orthogonal-curved contours ( $t_{(9)} = 5.43$ ,  $p = 0.001$ , Cohen's  $d = 1.72$ ; FDR-corrected), which shared the same contour type with training condition. Consistent with Experiment 1, the performance for collinear-straight contours ( $t_{(9)} = 0.85$ ,  $p = 0.503$ , Cohen's  $d = 0.27$ ; FDR-corrected) and collinear-curved contours ( $t_{(9)} = 0.34$ ,  $p = 0.743$ , Cohen's  $d = 0.11$ ; FDR-corrected) did not show significant improvement after training. Similarly, the MI of acute-straight contours ( $t_{(9)} = 1.49$ ,  $p = 0.257$ , Cohen's  $d = 0.47$ ; FDR-corrected) had no difference with 0. The difference between MI of acute- curved contours and 0 was marginally significant ( $t_{(9)} = 2.38$ ,  $p = 0.083$ , Cohen's  $d = 0.75$ ; FDR-corrected). These results showed that the learning effect was significant on training condition and could transfer to the untrained condition with trained type and untrained path, but lack of significant learning transfer to the other conditions, supporting the learning of contour type in contour-detection training. In addition, we did not observe significant difference in performance for orthogonal-straight contours between the posttest

I and the posttest II (threshold:  $t(9) = 0.66$ ,  $p = 0.525$ , Cohen's  $d = 0.21$ ), which indicated a prolonged learning effect (Figure 8C vs. Figure 8D).

*Partial transfer of learning effect across contour paths when training on the straight path*

A two-way (contour type  $\times$  contour path) repeated-measures ANOVA on the MI of threshold showed a main effect of contour type ( $F_{(2,18)} = 30.45$ ,  $p < 0.001$ ,  $\eta_p^2 = 0.77$ ). Post hoc test revealed that there was more performance improvement for the trained than untrained type (orthogonal vs. collinear:  $t_{(19)} = 6.27$ ,  $p < 0.001$ , Cohen's  $d = 2.61$ ; orthogonal vs. acute:  $t_{(19)} = 6.77$ ,  $p < 0.001$ , Cohen's  $d = 2.41$ ; FDR-corrected). The main effect of contour path ( $F_{(1,9)} = 15.64$ ,  $p = 0.003$ ,  $\eta_p^2 = 0.64$ ) and the interaction effects ( $F_{(2,18)} = 10.45$ ,  $p < 0.001$ ,  $\eta_p^2 = 0.54$ ) also reached significance level. Simple effect analysis showed that, only for orthogonal contours, the MI of straight paths was significant larger than that of curved paths ( $t_{(9)} = 5.11$ ,  $p < 0.001$ , Cohen's  $d = 1.62$ ). No significant difference of MI between different paths were observed for collinear contours ( $t_{(9)} = 0.39$ ,  $p = 0.709$ , Cohen's  $d = 0.12$ ) or acute contours ( $t_{(9)} = -0.29$ ,  $p = 0.780$ , Cohen's  $d = -0.09$ ). Furthermore, the TI of threshold for orthogonal-curved contours was significantly higher than 0 ( $t_{(9)} = 4.67$ ,  $p = 0.006$ , Cohen's  $d = 1.48$ ; FDR-corrected), but lower than 1 ( $t_{(9)} = -5.13$ ,  $p < 0.001$ , Cohen's  $d = -1.62$ ; FDR-corrected). None of the TI for other untrained conditions was significantly higher than 0. These results may indicate a partial transfer of contour-detection learning between paths but no transfer between types.

## Experiment 2b

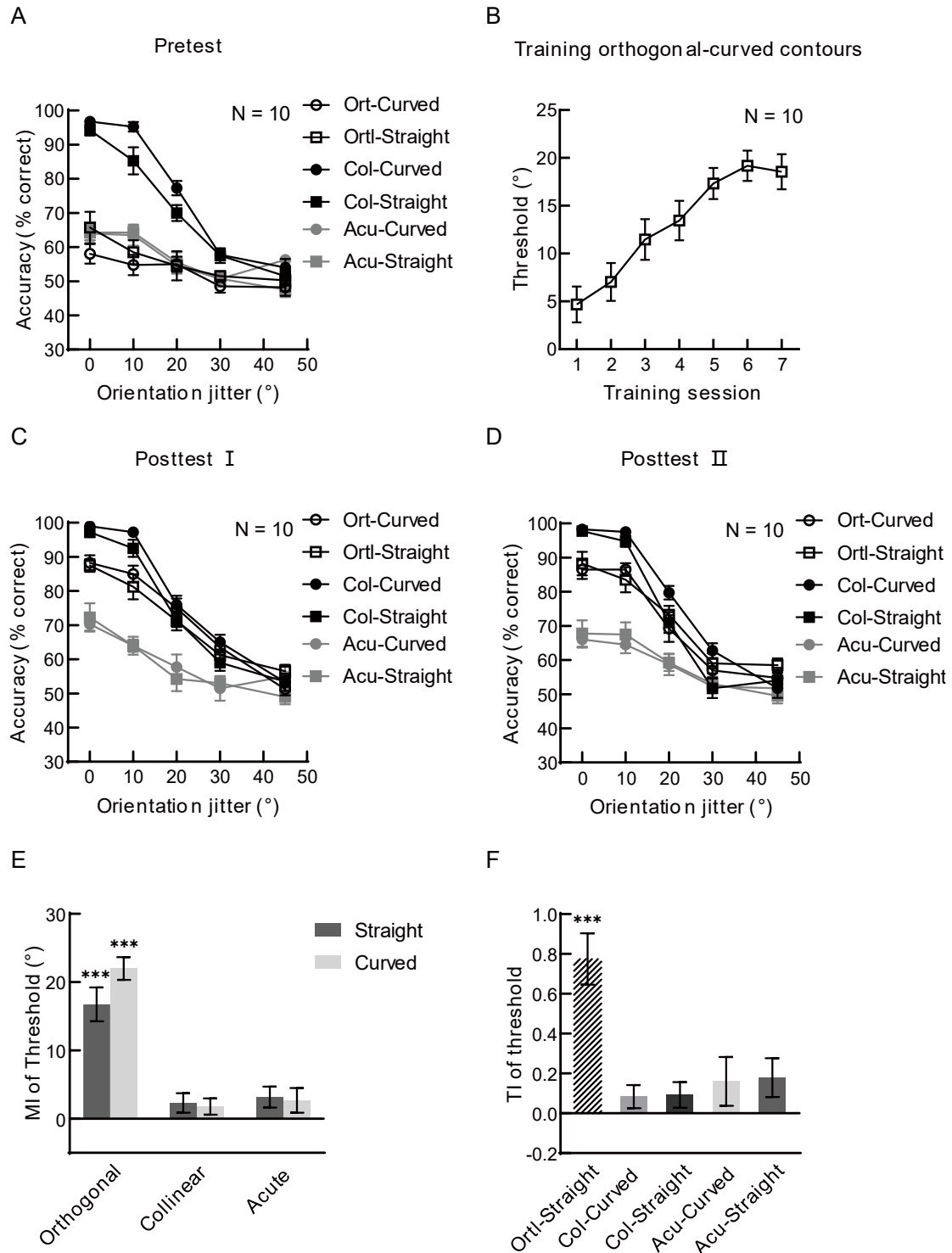


**Figure 9.** Training on Orthogonal-Curved Contours in Experiment 2b. (A) Psychometric curves (averaged across participants) for contour detection performance (percent correct) plotted as a function of local orientation jitter before training on orthogonal-curved contours. (B) Detection performance for each training session. (C) Psychometric curves for performance (percent correct) plotted as a function of local orientation jitter after training. (D) Psychometric curves for

performance (percent correct) tested 3-16 weeks after training. (E) MI of detection thresholds for trained and untrained conditions after training on orthogonal-curved contours. (F) TI of detection thresholds for untrained conditions. Asterisks indicate significant difference with 0. Error bars represent standard error of the mean across participants.

*Improved performance in detecting orthogonal contours both for trained and untrained path*

In Experiment 2b, one of eleven participants' detection accuracy for orthogonal-curved contours at 0° jitter in posttest I didn't reach 70%, for which data from this participant was not used in the analysis. As we observed in the above experiments, participants were more sensitive to collinear contours than orthogonal or acute contours before training (Figure 9A). In the training phase (Figure 9B), the threshold of the last session was significantly higher than that of the first session ( $t_{(9)} = 7.79, p < 0.001$ , Cohen's  $d = 2.46$ , and there was no significant difference between the thresholds of the last two sessions ( $t_{(9)} = -0.76, p = 0.468$ , Cohen's  $d = -0.24$ ), which indicated that the training reached the asymptotic level.

One-sample t-tests (two-tailed, compared with 0) on the MI of thresholds (Figure 9E) revealed significant improved performance for both orthogonal-curved (trained) contours ( $t_{(9)} = 13.13, p < 0.001$ , Cohen's  $d = 4.15$ ; FDR-corrected) and orthogonal-straight contours, the untrained condition with trained type but untrained path ( $t_{(9)} = 6.76, p < 0.001$ , Cohen's  $d = 2.14$ ; FDR-corrected). However, there was no significant improvement for other untrained conditions (collinear-straight contours:  $t_{(9)} = 1.63, p = 0.172$ , Cohen's  $d = 0.51$ ; collinear-curved contours:  $t_{(9)} = 1.48, p = 0.172$ , Cohen's  $d = 0.47$ ; acute-straight contours:  $t_{(9)} = 2.08, p = 0.136$ , Cohen's  $d = 0.66$ ; acute-curved contours:  $t_{(9)} = 1.49, p = 0.172$ , Cohen's  $d = 0.47$ ; FDR-corrected) after training. These results suggest that the contour-detection learning effect was transferable between contour paths but untransferable between contour types, supporting the argument that participants learned the image statistic regularity in contour stimuli during training.

*Near-complete transfer of learning effect across contour paths when training on the curved path*

A two-way (contour type  $\times$  contour path) repeated-measures ANOVA on the MI of threshold showed a significant main effect of contour type ( $F_{(2,18)} = 54.22, p < 0.001, \eta_p^2 = 0.86$ ). Post hoc test revealed that there was more improvement for orthogonal contours than collinear or acute contours (orthogonal vs. collinear:  $t_{(19)} = 9.25, p < 0.001$ , Cohen's  $d = 3.17$ ; orthogonal vs. acute:  $t_{(19)} = 8.77,$

$p < 0.001$ , Cohen's  $d = 3.01$ ; FDR-corrected). Moreover, The main effect of contour path ( $F_{(1,9)} = 3.92$ ,  $p = 0.079$ ,  $\eta_p^2 = 0.30$ ) and the interaction effect ( $F_{(2,18)} = 2.81$ ,  $p = 0.087$ ,  $\eta_p^2 = 0.24$ ) were marginally significant. Simple effect analysis showed that the difference between the MI of straight paths and curved paths was neither significant for collinear contours ( $t_{(9)} = 0.32$ ,  $p = 0.757$ , Cohen's  $d = 0.10$ ) nor acute contours ( $t_{(9)} = 0.39$ ,  $p = 0.705$ , Cohen's  $d = 0.12$ ), but significant for orthogonal contours ( $t_{(9)} = -2.35$ ,  $p = 0.043$ , Cohen's  $d = 0.74$ ). The MI for orthogonal-curved (trained) contours was significantly larger than that for orthogonal-straight (untrained) contours. However, the TI of threshold for untrained orthogonal-curved contours was significantly higher than 0 ( $t_{(9)} = 6.00$ ,  $p = 0.001$ , Cohen's  $d = 1.90$ ; FDR-corrected), but showed no significant difference with 1 ( $t_{(9)} = -1.75$ ,  $p = 0.115$ , Cohen's  $d = 0.55$ ; FDR-corrected). There was no significant difference between TI for other untrained conditions and 0. These results indicate that the improvement for the two conditions with trained contour type but different contour paths were similar, suggesting a near-complete learning transfer between paths. Furthermore, although the difference between performance for training condition in posttest I (Figure 9C) and posttest II (Figure 9D) was significant (threshold:  $t_{(9)} = -0.62$ ,  $p = 0.553$ , Cohen's  $d = -0.20$ ), participants' detection thresholds for training condition was significantly higher in posttest II than in pretest (threshold:  $t_{(9)} = 9.97$ ,  $p < 0.001$ , Cohen's  $d = 3.15$ ), indicating that the performance improvement after training could last for a relatively long time.

#### *The effects of training condition on the degree of learning transfer*

To compare the transfer effects among different training conditions, we further conducted an independent-sample t-test on TI of the condition with trained contour type and untrained contour path in Experiment 2a and Experiment 2b. The difference between TI in the two experiments was marginally significant ( $t_{(18)} = 1.81$ ,  $p = 0.087$ , Cohen's  $d = 0.81$ ). Furthermore, similar to Experiment 1, we also performed a mixed-design ANOVA on the MI of thresholds with contour type (collinear vs. orthogonal) and contour path (straight vs. curved) as within-subject factors and experiment (Experiment 2a and Experiment 2b) as a between-subject factor. The three-factor interaction ( $F_{(2,17)} = 1.10$ ,  $p = 0.354$ ,  $\eta_p^2 = 0.12$ ), the interaction between experiment and contour type ( $F_{(2,17)} = 0.76$ ,  $p = 0.482$ ,  $\eta_p^2 = 0.08$ ) and the main effect of experiment ( $F_{(1,18)} = 2.02$ ,  $p = 0.173$ ,  $\eta_p^2 = 0.10$ ) were not significant. The interaction between experiment and contour path was marginally significant ( $F_{(1,18)}$

= 4.21,  $p = 0.055$ ,  $\eta_p^2 = 0.19$ ), and other interactions and main effects were all significant (the contour type  $\times$  contour path interaction:  $F_{(2,17)} = 10.18$ ,  $p = 0.001$ ,  $\eta_p^2 = 0.55$ ; the main effect of contour type:  $F_{(2,17)} = 66.42$ ,  $p < 0.001$ ,  $\eta_p^2 = 0.89$ ; the main effect of contour path:  $F_{(1,18)} = 19.06$ ,  $p < 0.001$ ,  $\eta_p^2 = 0.51$ ). Simple analysis showed that there was no significant difference between performance improvement in Experiment 2a and Experiment 2b both for the trained contour path ( $t_{(58)} = 0.22$ ,  $p = 0.827$ , Cohen's  $d = 0.06$ ) and the untrained contour path ( $t_{(58)} = 1.53$ ,  $p = 0.130$ , Cohen's  $d = 0.40$ ). This result was not identical to what we observed in Experiment 1, which may be influenced by the different task difficulty and training duration in Experiment 2.

In sum, results in Experiment 1 and Experiment 2 suggested that the performance improvement was specific to the trained contour type but could transfer to the untrained contour path after contour-detection training. This indicated that participants could learn to use image regularities (organization regularities) in contour stimuli for contour linking during contour-detection training, which implied that this contour integration learning effect may be transferable over global feature dimensions of contour stimuli. However, a previous study (Zhang & Kourtzi, 2010) showed that the learning effect of contour detection was specific to global orientation. To examine whether the contour integration learning could transfer over global contour orientation or not, we performed Experiment 3 and Experiment 4.

## Experiment 3a

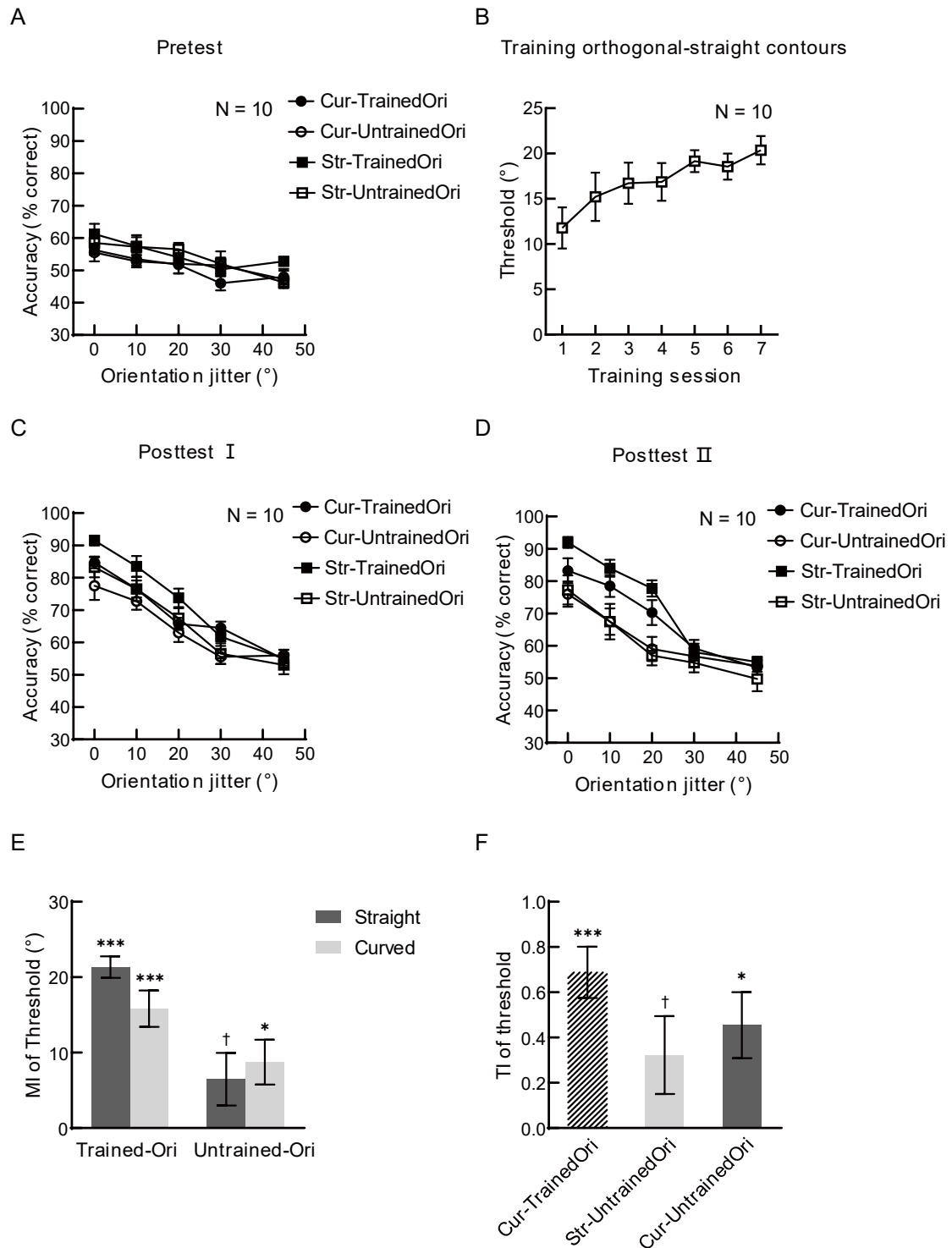


**Figure 10.** Training on Orthogonal-Straight Contours in Experiment 3a. (A) Psychometric curves (averaged across participants) for contour detection performance (percent correct) plotted as a function of local orientation jitter before training on orthogonal-straight contours. (B) Detection performance for each training session. (C) Psychometric curves for performance (percent correct) plotted as a function of local orientation jitter after training. (D) Psychometric curves for

performance (percent correct) tested 3-16 weeks after training. (E) MI of detection thresholds for trained and untrained conditions after training on orthogonal-straight contours. (F) TI of detection thresholds for untrained conditions. Asterisks indicate significant difference with 0. Error bars represent standard error of the mean across participants.

#### *Improved performance in detecting orthogonal contours after training*

In Experiment 3a, participants underwent training on orthogonal-straight contours orientated at 45° or 135°. Two of the twelve participants were excluded from the analysis for their detection accuracy at 0° jitter lower than the criterion. Figure 10A shows that observers' detection sensitivity for orthogonal contours with trained path (straight) or untrained path (curved) orientated at trained orientations or untrained orientations was at a chance level before training. During the training phase, participants' detection thresholds for the training condition increased across sessions (Figure 10B). Particularly, there was a significant difference between the thresholds of the first training session and the last training session ( $t_{(9)} = 5.58, p < 0.001$ , Cohen's  $d = 1.77$ ), but no significant difference between the thresholds of the last two sessions ( $t_{(9)} = 1.27, p = 0.236$ , Cohen's  $d = 0.40$ ).

Participants' performance immediately after training (posttest I) and 3-16 weeks after training (posttest II) are shown in Figure 10C and Figure 10D, respectively. There was no significant difference in performance for the trained condition (orthogonal-straight contours orientated at trained orientations) between posttest I and posttest II (threshold:  $t_{(9)} = -0.26, p = 0.802$ , Cohen's  $d = -0.08$ ). Figure 10E shows the mean improvements (posttest I – pretest) of contour detection thresholds for trained and untrained conditions. One-sample t-tests (two-tailed, compared with 0) on the MI of thresholds after training showed significant improvements for straight (trained path) contours orientated at trained orientations ( $t_{(9)} = 14.94, p < 0.001$ , Cohen's  $d = 4.73$ ; FDR-corrected) and curved (untrained path) contours orientated at trained orientations ( $t_{(9)} = 6.55, p < 0.001$ , Cohen's  $d = 2.07$ ; FDR-corrected). Furthermore, significant improvement was also observed for curved contours orientated at untrained orientations ( $t_{(9)} = 2.94, p = 0.022$ , Cohen's  $d = 0.93$ ; FDR-corrected), and a trend of significant improvement was observed for straight contours orientated at untrained orientations ( $t_{(9)} = 1.87, p = 0.095$ , Cohen's  $d = 0.59$ ; FDR-corrected). These results suggest that the learning effect for orthogonal-straight contours could last a prolonged period and may transfer to the untrained contour path and even untrained contour orientation.

#### *Partial transfer of learning effect across both contour paths and contour orientations when*

### *training on the straight path*

We further conducted a two-way (contour path  $\times$  contour orientation) repeated-measures ANOVA on the MI of threshold, which revealed a significant main effect of contour orientation ( $F_{(1,9)} = 10.62, p = 0.010, \eta_p^2 = 0.54$ ) and a significant interaction between contour path and contour orientation ( $F_{(1,9)} = 5.63, p = 0.042, \eta_p^2 = 0.39$ ). However, the main effect of the contour path was not significant ( $F_{(1,9)} = 0.75, p = 0.408, \eta_p^2 = 0.08$ ). Simple effect analysis for the contour path showed that improvement in detecting straight (trained) paths was significantly larger than that in detecting curved (untrained) paths for contours orientated at trained orientation ( $t_{(9)} = 2.87, p = 0.019$ , Cohen's  $d = 0.91$ ), and there was no significant difference in improvements between straight paths and contour paths for contours orientated at untrained orientation ( $t_{(9)} = -0.77, p = 0.462$ , Cohen's  $d = -0.24$ ). Simple effect analysis for the contour orientation revealed a significant higher improvement for contours orientated at trained orientations than contours orientated at untrained orientations ( $t_{(9)} = 3.61, p = 0.006$ , Cohen's  $d = 1.14$ ) when contour paths were straight (trained). The difference in improvements between curved (untrained) contours orientated at trained orientations and curved (untrained) contours orientated at untrained orientations showed a trend towards significance ( $t_{(9)} = 2.13, p = 0.062$ , Cohen's  $d = 0.67$ ).

Furthermore, one-sample t-tests revealed that the TI of thresholds for untrained conditions were significantly higher than 0 (curved contours orientated at trained orientations:  $t_{(9)} = 7.77, p < 0.001$ , Cohen's  $d = 2.46$ ; FDR-corrected; curved contours orientated at untrained orientations:  $t_{(9)} = 3.15, p = 0.018$ , Cohen's  $d = 1.00$ ; FDR-corrected) or showed a trend higher than 0 (straight contours orientated at untrained orientations:  $t_{(9)} = 1.94, p = 0.084$ , Cohen's  $d = 0.613$ ; FDR-corrected). However, the TI of threshold for all untrained conditions were significantly lower than 1 (curved contours orientated at trained orientations:  $t_{(9)} = -2.93, p = 0.017$ , Cohen's  $d = -0.9$ ; straight contours orientated at untrained orientations:  $t_{(9)} = -3.67, p = 0.008$ , Cohen's  $d = -1.16$ ; curved contours orientated at untrained orientations:  $t_{(9)} = -4.23, p = 0.007$ , Cohen's  $d = -1.34$ ; FDR-corrected). These results may imply the partial transfer of contour detection learning between both contour paths and contour orientations.

## Experiment 3b

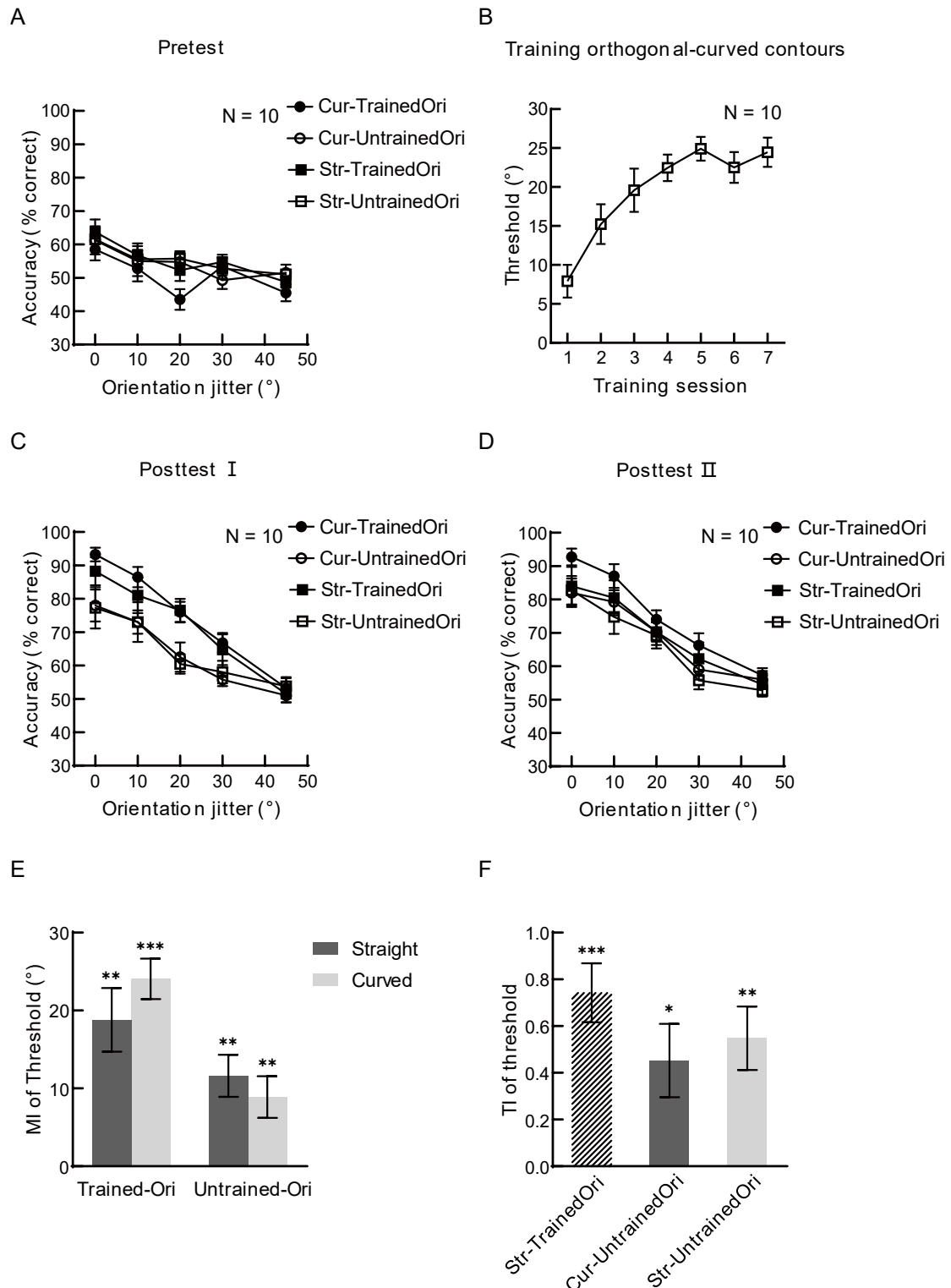


**Figure 11.** Training on Orthogonal-Curved Contours in Experiment 3b. (A) Psychometric curves (averaged across participants) for contour detection performance (percent correct) plotted as a function of local orientation jitter before training on orthogonal-curved contours. (B) Detection performance for each training session. (C) Psychometric curves for performance (percent correct)

plotted as a function of local orientation jitter after training. (D) Psychometric curves for performance (percent correct) tested 3-16 weeks after training. (E) MI of detection thresholds for trained and untrained conditions after training on orthogonal-curved contours. (F) TI of detection thresholds for untrained conditions. Asterisks indicate significant difference with 0. Error bars represent standard error of the mean across participants.

#### *Improved performance in detecting orthogonal contours after training*

In Experiment 3b, we trained participants to detect orthogonal-curved contours orientated at 45° or 135°. Before training, the detection performance of participants for all conditions was not significantly different from chance (Figure 11A). Participants' detection thresholds for the training condition increased during the training phase (Figure 11B). There was a significant improvement in thresholds between the last training session and the first training session ( $t_{(9)} = 7.84, p < 0.001$ , Cohen's  $d = 2.48$ ). There was no significant difference between thresholds in the last session and the third session ( $t_{(9)} = -0.36, p = 0.728$ , Cohen's  $d = -0.11$ ), but the difference in thresholds between the last two sessions was significant ( $t_{(9)} = 2.56, p = 0.031$ , Cohen's  $d = 0.81$ ). Furthermore, we did not observe a significant difference in detection thresholds for the training condition between the last training session in Experiment 3b and Experiment 3a ( $t_{(18)} = 1.68, p = 0.111$ , Cohen's  $d = 0.75$ ), indicating that the degree of training on orthogonal-curved contours and that on orthogonal-straight contours were at the same level. Figure 11C and Figure 11D show the detection performance of participants for posttest I (immediately after training) and posttest II (3-16 weeks after training) in Experiment 3b, respectively. There was no significant difference in performance for the trained condition (orthogonal-curved contours orientated at trained orientations) between the two posttest phases (threshold:  $t_{(9)} = 1.08, p = 0.309$ , Cohen's  $d = 0.34$ ).

To evaluate the learning effect of contour detection, we calculated mean improvements (posttest I – pretest) of detection thresholds for trained and untrained conditions in the current experiment (Figure 11E). One-sample t-tests (two-tailed, compared with 0) on the MI showed significant improvements for all conditions (curved contours orientated at trained orientations:  $t_{(9)} = 9.25, p < 0.001$ , Cohen's  $d = 2.93$ ; straight contours orientated at trained orientations:  $t_{(9)} = 4.60, p = 0.003$ , Cohen's  $d = 1.45$ ; curved contours orientated at untrained orientations:  $t_{(9)} = 3.32, p = 0.009$ , Cohen's  $d = 1.05$ ; straight contours orientated at untrained orientations:  $t_{(9)} = 4.30, p = 0.003$ , Cohen's  $d = 1.36$ ; FDR-corrected) after training, indicating a significant learning effect for training condition and transfers of learning across both contour paths and contour orientations.

*Near-complete transfer of learning effect across contour paths and partial transfer across contour orientations when training on the curved path*

A two-way (contour path  $\times$  contour orientation) repeated-measures ANOVA on the MI of threshold showed a significant main effect of contour orientation ( $F_{(1,9)} = 5.12, p = 0.050, \eta_p^2 = 0.36$ ) and a significant interaction effect ( $F_{(1,9)} = 8.04, p = 0.020, \eta_p^2 = 0.47$ ) but no significant main effect of contour path ( $F_{(1,9)} = 0.65, p = 0.440, \eta_p^2 = 0.07$ ). Simple effect analysis for contour path revealed a trend of significantly higher MI for curved (trained) paths than straight (untrained) paths when contours orientated at trained orientations ( $t_{(9)} = 2.12, p = 0.063, \text{Cohen's } d = 0.67$ ), but no significant difference between them when contours orientated at untrained orientations ( $t_{(9)} = -1.65, p = 0.134, \text{Cohen's } d = 0.52$ ). Simple effect analysis for contour orientation revealed only for curved (trained) contours was the MI in detecting trained orientations significantly higher than that in detecting untrained orientations ( $t_{(9)} = 3.35, p = 0.009, \text{Cohen's } d = 1.06$ ).

Moreover, One-sample t-tests on the TI of thresholds for three untrained conditions (Figure. 11F) revealed that they were significantly higher than 0 (straight contours orientated at trained orientations:  $t_{(9)} = 5.86, p < 0.001, \text{Cohen's } d = 1.8$ ; curved contours orientated at untrained orientations:  $t_{(9)} = 2.88, p = 0.018, \text{Cohen's } d = 0.9$ ; straight contours orientated at untrained orientations:  $t_{(9)} = 4.03, p = 0.004, \text{Cohen's } d = 1.27$ ; FDR-corrected) but significantly lower or in a trend of significantly lower than 1 (straight contours orientated at trained orientations:  $t_{(9)} = -2.03, p = 0.073, \text{Cohen's } d = -0.64$ ; curved contours orientated at untrained orientations:  $t_{(9)} = -3.49, p = 0.013, \text{Cohen's } d = -1.10$ ; straight contours orientated at untrained orientations:  $t_{(9)} = -3.32, p = 0.013, \text{Cohen's } d = -1.05$ ; FDR-corrected). These results indicate the learning effect for contour detection could partially transfer to untrained path and untrained orientation, which may support the learning of image regularity in contour stimuli during contour detection training.

*No effects of training condition on the pattern of learning transfer*

To compare the transfer effect of learning between Experiment 3a (training on orthogonal-straight contours) and Experiment 3b (training on orthogonal-curved contours), we applied a mixed-design ANOVA to the TI of thresholds with contour condition (three untrained conditions) as a within-subject factor and experiment (Experiment 3a and Experiment 3b) as a between-subject factor. Neither the main effect of experiment ( $F_{(1,18)} = 0.33, p = 0.574, \eta_p^2 = 0.02$ ) nor the interaction effect ( $F_{(2,36)} = 0.11, p = 0.893, \eta_p^2 = 0.01$ ) was significant, suggesting there was no significant

difference in transfer effect between different training conditions (straight contours vs. curved contours).

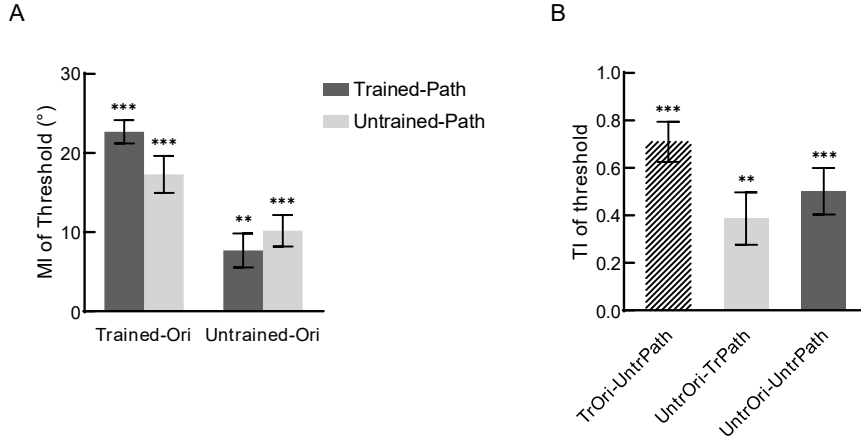


Figure 12. Performance Improvement for Orthogonal Contours in Experiment 3. (A) MI of detection thresholds for trained and untrained conditions after training on orthogonal-straight contours or orthogonal-curved contours. (B) TI of detection thresholds for untrained conditions. Asterisks indicate significant difference with 0. Error bars represent standard error of the mean across participants.

We further combined Experiment 3a and Experiment 3b since a mixed-design ANOVA (experiment  $\times$  contour path  $\times$  contour orientation) on the MI revealed no significant difference between performance improvement patterns in Experiment 3a and Experiment 3b (experiment  $\times$  contour path  $\times$  contour orientation:  $F_{(1,18)} = 0.003$ ,  $p = 0.955$ ,  $\eta_p^2 = 0$ ; experiment  $\times$  contour path:  $F_{(1,18)} = 0.02$ ,  $p = 0.955$ ,  $\eta_p^2 = 0.001$ ; experiment  $\times$  contour orientation:  $F_{(1,18)} = 0.001$ ,  $p = 0.973$ ,  $\eta_p^2 = 0$ ; the main effect of experiment:  $F_{(1,18)} = 1.48$ ,  $p = 0.39$ ,  $\eta_p^2 = 0.08$ ). The pooled results ( $n = 20$ ) showed significant improvements for all four orthogonal-contour conditions (one-sample t-tests, compared with 0; trained-path  $\times$  trained-orientation:  $t_{(19)} = 15.36$ ,  $p < 0.001$ , Cohen's  $d = 3.43$ ; untrained-path  $\times$  trained-orientation:  $t_{(19)} = 7.41$ ,  $p < 0.001$ , Cohen's  $d = 1.66$ ; trained-path  $\times$  untrained-orientation:  $t_{(19)} = 3.57$ ,  $p = 0.002$ , Cohen's  $d = 0.80$ ; untrained-path  $\times$  untrained-orientation:  $t_{(19)} = 5.13$ ,  $p < 0.001$ , Cohen's  $d = 1.15$ ; FDR-corrected; Figure. 12A). Two-way (contour path  $\times$  contour orientation) repeated-measures ANOVA on the MI revealed a significant interaction effect ( $F_{(1,19)} = 14.05$ ,  $p = 0.001$ ,  $\eta_p^2 = 0.43$ ) and a significant main effect of contour orientation ( $F_{(1,9)} = 14.48$ ,  $p = 0.001$ ,  $\eta_p^2 = 0.43$ ) but no significant main effect of contour path ( $F_{(1,9)} = 1.48$ ,  $p = 0.239$ ,  $\eta_p^2 = 0.07$ ). Simple effect analysis for contour path revealed significantly higher

MI for trained paths compared to untrained paths when contours orientated at trained orientations only ( $t_{(19)} = 3.52$ ,  $p = 0.002$ , Cohen's  $d = 0.79$ ). Simple effect analysis for contour orientation revealed significantly higher MI in detecting contours orientated at trained orientations than in detecting contours orientated at untrained orientations, no matter the paths of contours were trained ( $t_{(19)} = 5.04$ ,  $p < 0.001$ , Cohen's  $d = 1.13$ ) or untrained ( $t_{(19)} = 2.23$ ,  $p = 0.038$ , Cohen's  $d = 0.50$ ). One-sample t-tests on the combined data showed that the TI of the three untrained orthogonal-contour conditions were significantly higher than 0 (untrained-path  $\times$  trained-orientation:  $t_{(19)} = 9.58$ ,  $p < 0.001$ , Cohen's  $d = 2.14$ ; trained-path  $\times$  untrained-orientation:  $t_{(19)} = 3.43$ ,  $p = 0.003$ , Cohen's  $d = 0.77$ ; untrained-path  $\times$  untrained-orientation:  $t_{(19)} = 5.16$ ,  $p < 0.001$ , Cohen's  $d = 1.15$ ; FDR-corrected; Figure. 12B) but lower than 1 (untrained-path  $\times$  trained-orientation:  $t_{(19)} = -3.47$ ,  $p = 0.003$ , Cohen's  $d = -0.78$ ; trained-path  $\times$  untrained-orientation:  $t_{(19)} = -5.17$ ,  $p < 0.001$ , Cohen's  $d = -1.16$ ; untrained-path  $\times$  untrained-orientation:  $t_{(19)} = -5.42$ ,  $p < 0.001$ , Cohen's  $d = -1.21$ ; FDR-corrected). These results indicated the transfer of contour detection learning between contour paths and between contour orientations.

To confirm the performance improvements for contours with untrained path or untrained orientation in Experiment 3a and Experiment 3b were due to the learning of image regularities in contour stimuli and excluded the influence of familiarity with the task procedure, we trained participants on orthogonal contours and tested them on both orthogonal and acute contours in Experiment 4a and Experiment 4b.

## Experiment 4a

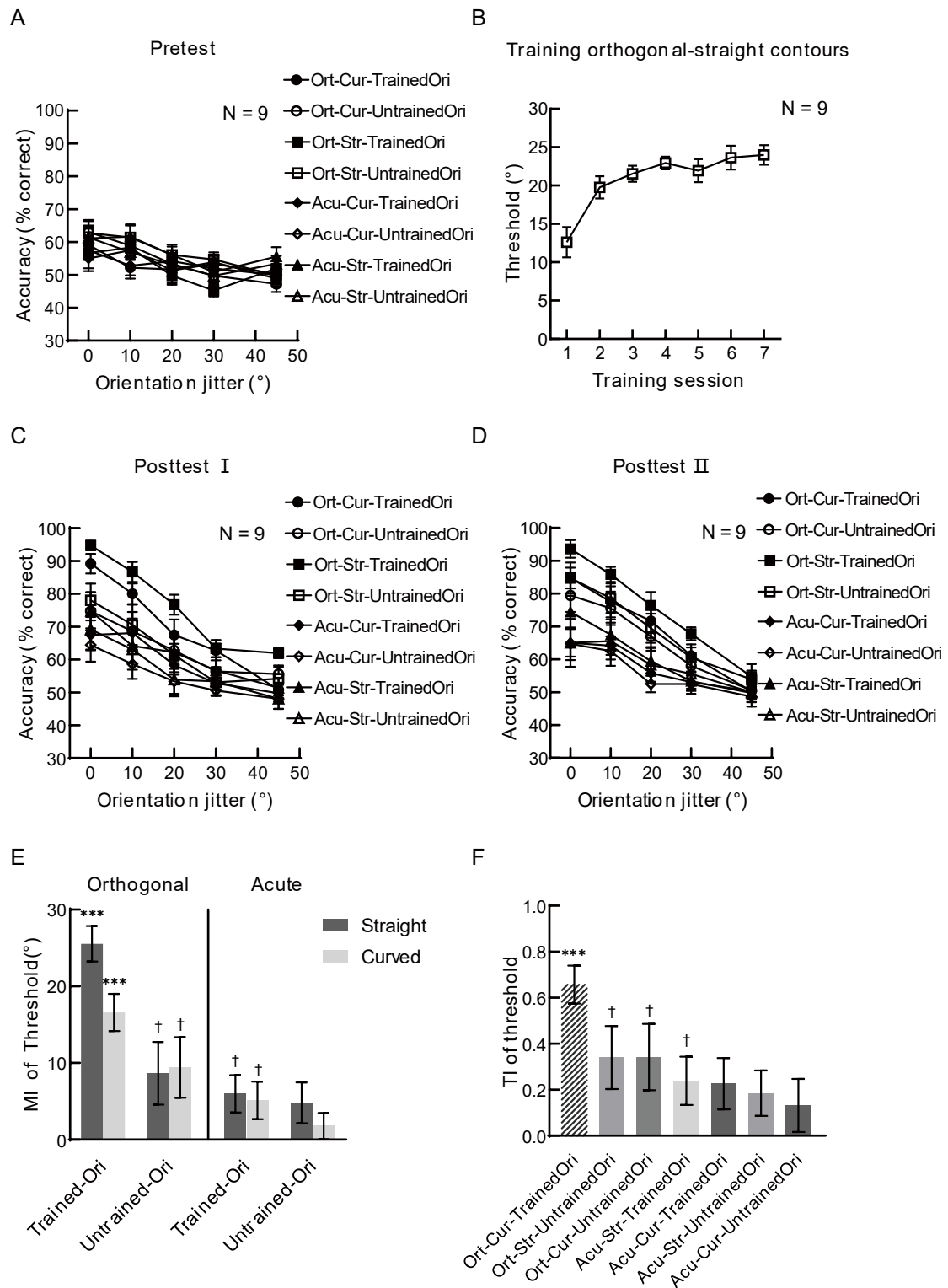


**Figure 13.** Training on Orthogonal-Straight Contours in Experiment 4a. (A) Psychometric curves (averaged across participants) for contour detection performance (percent correct) plotted as a function of local orientation jitter before training on orthogonal-straight contours. (B) Detection performance for each training session. (C) Psychometric curves for performance (percent correct)

plotted as a function of local orientation jitter after training. (D) Psychometric curves for performance (percent correct) tested 3-16 weeks after training. (E) MI of detection thresholds for trained and untrained conditions after training on orthogonal-straight contours. (F) TI of detection thresholds for untrained conditions. Asterisks indicate significant difference with 0. Error bars represent standard error of the mean across participants.

#### *Improved performance in detecting orthogonal contours after training*

In Experiment 4a, we trained participants on orthogonal-straight contours orientated at 45° or 135° and tested them on orthogonal and acute contours with trained or untrained path orientated at trained or untrained orientation. Data of one participant who failed to achieve the criterion detection performance after seven training sessions were excluded from the analysis. As shown in Figure. 13A, participants' detection performance for all orthogonal or acute contours conditions was not significantly different from chance before training. During the training phase, the detection thresholds of participants gradually increased (Figure. 13B), and there was no significant difference in thresholds between the last two training sessions ( $t_{(8)} = 0.46, p = 0.656, \text{Cohen's } d = 0.15$ ). Figure. 13C and Figure. 13D show the performance of participants in posttest I and posttest II, respectively. The difference between detection thresholds for the trained condition in the two posttest phases was not significant (threshold:  $t_{(8)} = -0.03, p = 0.980, \text{Cohen's } d = -0.01$ ).

Figure. 13E shows the mean improvements (posttest I – pretest) of contour detection thresholds for trained and untrained conditions after training. One-sample t-tests (two-tailed, compared with 0) on the MI of thresholds for all eight conditions revealed a significant improvement for orthogonal-straight (trained) contours orientated at trained orientations ( $t_{(8)} = 11.03, p < 0.001, \text{Cohen's } d = 3.68; \text{FDR-corrected}$ ) and orthogonal-curved (untrained) contours orientated at trained orientations ( $t_{(8)} = 6.84, p < 0.001, \text{Cohen's } d = 2.28; \text{FDR-corrected}$ ). The improvements for orthogonal-straight ( $t_{(8)} = 2.12, p = 0.093, \text{Cohen's } d = 0.71; \text{FDR-corrected}$ ) and orthogonal-curved ( $t_{(8)} = 2.38, p = 0.090, \text{Cohen's } d = 0.79; \text{FDR-corrected}$ ) contours orientated at untrained orientations were marginally significant. We also observed marginally significant improvements for acute-straight ( $t_{(8)} = 2.46, p = 0.090, \text{Cohen's } d = 0.82; \text{FDR-corrected}$ ) and acute-curved ( $t_{(8)} = 2.09, p = 0.093, \text{Cohen's } d = 0.70; \text{FDR-corrected}$ ) contours orientated at trained orientations, but no significant improvements for acute-straight ( $t_{(8)} = 1.81, p = 0.0124, \text{Cohen's } d = 0.60; \text{FDR-corrected}$ ) and acute-curved ( $t_{(8)} = 1.04, p = 0.327, \text{Cohen's } d = 0.35; \text{FDR-corrected}$ ) contours orientated at untrained orientations. These results indicated there was a transfer of learning effect between

contour paths.

*Partial transfer of learning effect between contour paths when training on straight path*

A three-way (contour type  $\times$  contour path  $\times$  contour orientation) repeated-measures ANOVA on the MI of thresholds showed a marginally significant interaction among contour type, contour path and contour orientation ( $F_{(1,8)} = 3.90, p = 0.084, \eta_p^2 = 0.33$ ). A further two-way (contour path  $\times$  contour orientation) repeated-measures ANOVA on the MI for orthogonal (trained type) contours revealed significant main effects of contour path ( $F_{(1,8)} = 7.60, p = 0.025, \eta_p^2 = 0.49$ ) and contour orientation ( $F_{(1,8)} = 16.76, p = 0.003, \eta_p^2 = 0.68$ ) and a significant interaction between path and orientation ( $F_{(1,8)} = 6.43, p = 0.035, \eta_p^2 = 0.45$ ). Simple effect analysis of contour path showed that the improvement in detecting straight (trained) paths was significantly higher than that in detecting curved (untrained) paths ( $t_{(8)} = 4.36, p = 0.002, \text{Cohen's } d = 1.45$ ), only for orthogonal contours orientated at trained orientations. For orthogonal contours orientated at untrained orientations, there was no significant difference in improvement between straight paths and curved paths ( $t_{(8)} = -0.27, p = 0.791, \text{Cohen's } d = -0.09$ ). Simple effect analysis of contour orientation showed a significant higher improvement in detecting contours orientated at trained orientations compared with detecting contours orientated at untrained orientations for orthogonal-straight (trained) contours ( $t_{(8)} = 4.45, p = 0.002, \text{Cohen's } d = 1.48$ ), and a trend of significant difference between the improvement of detecting trained orientations and that of detecting untrained orientations for orthogonal-curved (untrained) contours ( $t_{(8)} = 2.24, p = 0.055, \text{Cohen's } d = 0.75$ ). The two-way (contour path  $\times$  contour orientation) repeated-measures ANOVA on the MI for acute (untrained type) contours showed none of the main effects or the interaction effect was significant (the main effect of path:  $F_{(1,8)} = 1.15, p = 0.316, \eta_p^2 = 0.13$ ; the main effect of orientation:  $F_{(1,8)} = 0.48, p = 0.508, \eta_p^2 = 0.06$ ; the interaction effect:  $F_{(1,8)} = 0.40, p = 0.546, \eta_p^2 = 0.05$ ).

TI of thresholds for untrained conditions are shown in Figure. 13F. One-sample t-tests (two-tailed, compared with 0 and 1) showed the TI for untrained conditions were all significantly lower than 1. Only for orthogonal-curved contours orientated at trained orientations was the TI significantly higher than 0 ( $t_{(8)} = 7.95, p < 0.001, \text{Cohen's } d = 2.65; \text{FDR-corrected}$ ). The difference between TI for orthogonal-straight contours orientated at untrained orientations and 0 ( $t_{(8)} = 2.48, p = 0.093, \text{Cohen's } d = 0.83; \text{FDR-corrected}$ ) and that between orthogonal-curved contours orientated

at untrained orientations and 0 ( $t_{(8)} = 2.37, p = 0.093$ , Cohen's  $d = 0.79$ ; FDR-corrected) were marginally significant. The difference between TI for acute-straight contours orientated at trained orientations and 0 was also marginally significant ( $t_{(8)} = 2.27, p = 0.093$ , Cohen's  $d = 0.76$ ; FDR-corrected). None of the TI for other untrained conditions was significantly higher than 0.

To rule out the potential impact of familiarity with the task procedure and confirm the transfer of learning effect between paths or between orientations, we calculated the difference between MI for orthogonal-contour conditions and corresponding acute-contour conditions (Figure. 15A). One-sample t-tests (two-tailed, compared with 0) on the difference between MI showed significant improvement for contours orientated at trained orientations (trained-path (straight)  $\times$  trained-orientation:  $t_{(8)} = 5.79, p = 0.002$ , Cohen's  $d = 1.93$ ; untrained-path (curved)  $\times$  trained-orientation:  $t_{(8)} = 3.47, p = 0.017$ , Cohen's  $d = 1.16$ ; FDR-corrected), but no significant improvement for contours orientated at untrained orientations (trained-path (straight)  $\times$  untrained-orientation:  $t_{(8)} = 0.71, p = 0.499$ , Cohen's  $d = 0.24$ ; untrained-path (curved)  $\times$  untrained-orientation:  $t_{(8)} = 1.56, p = 0.20$ , Cohen's  $d = 0.52$ ; FDR-corrected). Two-way (contour path  $\times$  contour orientation) repeated-measures ANOVA revealed marginally significant interaction effect ( $F_{(1,8)} = 3.90, p = 0.084, \eta_p^2 = 0.33$ ) and main effect of contour orientation ( $F_{(1,8)} = 3.93, p = 0.083, \eta_p^2 = 0.33$ ), but no significant main effect of contour path ( $F_{(1,8)} = 0.68, p = 0.434, \eta_p^2 = 0.08$ ). Simple effect analysis showed significant higher improvement for contours with trained paths compared to contours with untrained paths only when contours orientated at trained orientations ( $t_{(8)} = 3.20, p = 0.013$ , Cohen's  $d = 1.07$ ), and significant higher improvement for contours orientated at trained orientations compared to contours orientated at untrained orientations only when contour paths were trained ( $t_{(8)} = 2.53, p = 0.035$ , Cohen's  $d = 0.84$ ). These results indicated the partial transfer of contour detection learning between contour paths, consistent with our findings in previous experiment.

## Experiment 4b

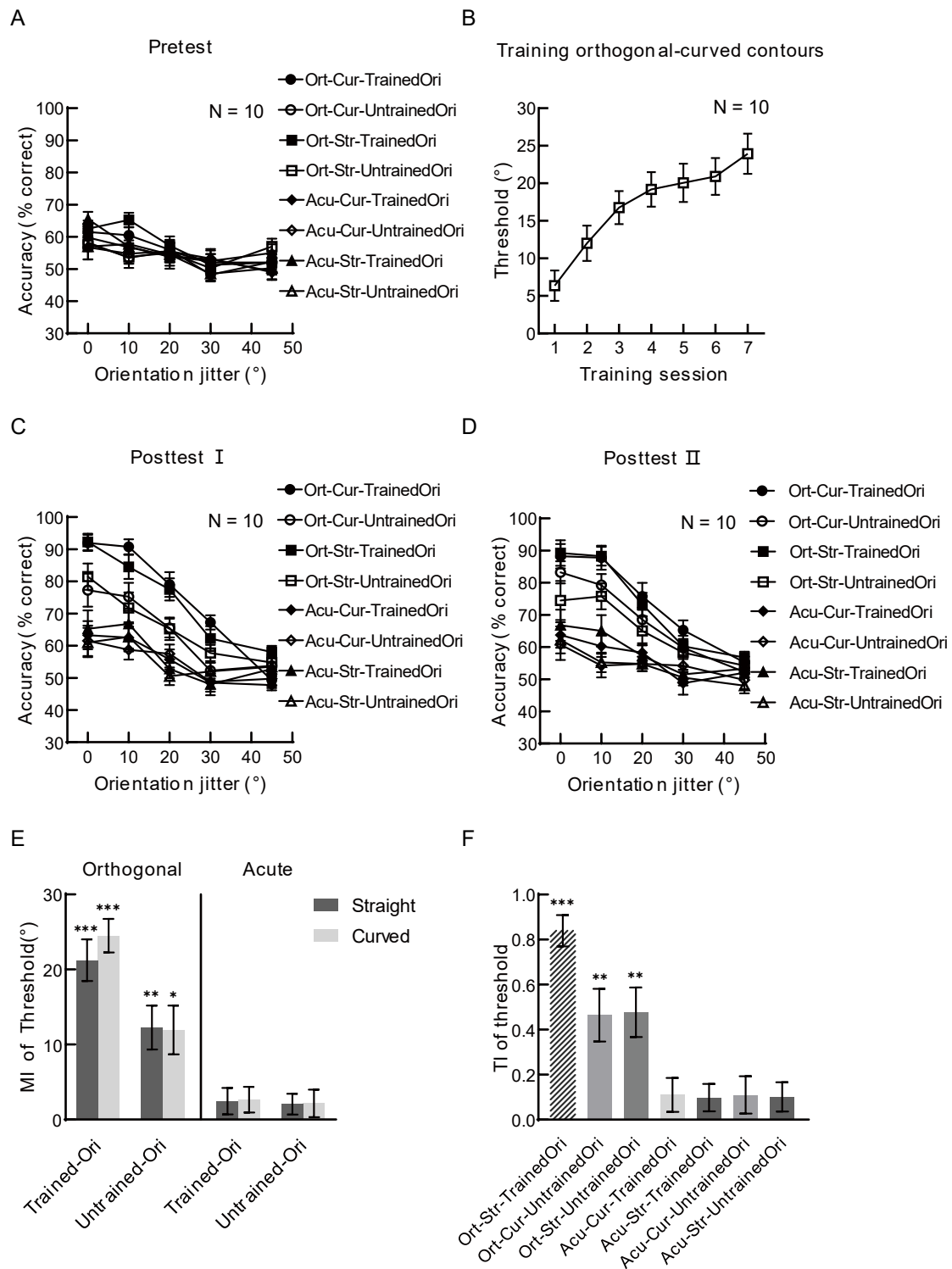


**Figure 14.** Training on Orthogonal-Curved Contours in Experiment 4b. (A) Psychometric curves (averaged across participants) for contour detection performance (percent correct) plotted as a function of local orientation jitter before training on orthogonal-curved contours. (B) Detection performance for each training session. (C) Psychometric curves for performance (percent correct) plotted as a function of local orientation jitter after training. (D) Psychometric curves for

performance (percent correct) tested 3-16 weeks after training. (E) MI of detection thresholds for trained and untrained conditions after training on orthogonal-curved contours. (F) TI of detection thresholds for untrained conditions. Asterisks indicate significant difference with 0. Error bars represent standard error of the mean across participants.

#### *Improved performance in detecting orthogonal contours after training*

In Experiment 4b, participants were trained on orthogonal-curved contours orientated at 45° or 135° and tested on both orthogonal contours and acute contours. Consistent with Experiment 3, participants' performance in detecting orthogonal and acute contours before training was at the chance level (Figure. 14A). As shown in Figure. 14B, participants' detection thresholds for the training condition gradually increased across training sessions. There was no significant difference between the threshold for the training condition of the last training session in Experiment 4b and that in Experiment 4a ( $t_{(17)} = -0.01, p = 0.990$ , Cohen's  $d = -0.006$ ), indicating participants reached an identical training level in the two experiments. Figure. 14C and Figure. 14D show participants' performance in posttest I and posttest II, respectively. No significant difference between detection thresholds for training condition in the two posttest phases was observed (threshold:  $t_{(9)} = 1.49, p = 170$ , Cohen's  $d = 0.47$ ).

As we did in the above experiments, we calculated the MI (posttest I – pretest) of thresholds for trained and untrained conditions after training (Figure. 14E). One-sample t-tests (two-tailed, compared with 0) on the MI revealed that there were significant performance improvements for all orthogonal-contour conditions (orthogonal-curved contours orientated at trained orientations:  $t_{(9)} = 10.96, p < 0.001$ , Cohen's  $d = 3.47$ ; orthogonal-straight contours orientated at trained orientations  $t_{(9)} = 7.65, p < 0.001$ , Cohen's  $d = 2.42$ ; orthogonal-curved contours orientated at untrained orientations:  $t_{(9)} = 3.67, p = 0.010$ , Cohen's  $d = 1.16$ ; orthogonal-straight contours orientated at untrained orientations  $t_{(9)} = 4.19, p = 0.006$ , Cohen's  $d = 1.33$ ; FDR-corrected), but no significant performance improvements for acute-contour conditions (acute-curved contours orientated at trained orientations:  $t_{(9)} = 1.54, p = 0.228$ , Cohen's  $d = 0.49$ ; acute -straight contours orientated at trained orientations  $t_{(9)} = 1.39, p = 0.228$ , Cohen's  $d = 0.44$ ; acute-curved contours orientated at untrained orientations:  $t_{(9)} = 1.17, p = 0.273$ , Cohen's  $d = 0.3$ ; acute -straight contours orientated at untrained orientations:  $t_{(9)} = 1.48, p = 0.228$ , Cohen's  $d = 0.47$ ; FDR-corrected). These results suggested that the learning effect for training condition was significant and could transfer to contours with same contour type but different contour path or different orientation.

*Near-complete transfer of learning effect between contour paths and partial transfer between orientations when training on curved contours*

We also applied three-way (contour type  $\times$  contour path  $\times$  contour orientation) repeated-measures ANOVA on the MI of thresholds, which revealed no significant three-factor interaction ( $F_{(1,9)} = 1.63, p = 0.234, \eta_p^2 = 0.15$ ), but a significant contour type  $\times$  contour orientation interaction ( $F_{(1,9)} = 45.96, p < 0.001, \eta_p^2 = 0.84$ ) and significant main effects of contour type ( $F_{(1,9)} = 25.07, p < 0.001, \eta_p^2 = 0.74$ ) and contour orientation ( $F_{(1,9)} = 9.01, p = 0.015, \eta_p^2 = 0.50$ ). None of the other effects reached significance. A further two-way (contour type  $\times$  contour orientation) repeated-measures ANOVA showed significant main effects of contour type ( $F_{(1,19)} = 51.64, p < 0.001, \eta_p^2 = 0.73$ ) and contour orientation ( $F_{(1,19)} = 16.95, p < 0.001, \eta_p^2 = 0.47$ ). The interaction effect was also significant ( $F_{(1,19)} = 49.44, p < 0.001, \eta_p^2 = 0.72$ ). Simple effect analysis showed that the performance improvement in detecting contours orientated at trained orientations was significantly higher than that of detecting contours orientated at untrained orientations for orthogonal contours ( $t_{(19)} = 5.77, p < 0.001, \text{Cohen's } d = 1.29$ ), but not for acute contours ( $t_{(19)} = 0.38, p = 0.703, \text{Cohen's } d = 0.09$ ). The improvement of orthogonal contours was significantly higher than that of acute contours, regardless of whether the contour orientation was trained ( $t_{(19)} = 9.84, p < 0.001, \text{Cohen's } d = 2.20$ ) or untrained ( $t_{(19)} = 4.18, p < 0.001, \text{Cohen's } d = 0.94$ ).

Figure. 14F shows the TI of thresholds for untrained conditions in the current experiment. We compared the TI with 0 and 1 respectively, using one-sample t-tests (two-tailed). TI for untrained orthogonal contours were significantly higher than 0 (orthogonal-straight contours orientated at trained orientations:  $t_{(9)} = 12.09, p < 0.001, \text{Cohen's } d = 3.82$ ; orthogonal-curved contours orientated at untrained orientations:  $t_{(9)} = 3.97, p = 0.008, \text{Cohen's } d = 1.26$ ; orthogonal-straight contours orientated at untrained orientations:  $t_{(9)} = 4.34, p = 0.007, \text{Cohen's } d = 1.37$ ; FDR-corrected) but lower than 1 (orthogonal-straight contours orientated at trained orientations:  $t_{(9)} = -2.32, p = 0.046, \text{Cohen's } d = -0.73$ ; orthogonal-curved contours orientated at untrained orientations:  $t_{(9)} = -4.59, p = 0.002, \text{Cohen's } d = -1.45$ ; orthogonal-straight contours orientated at untrained orientations:  $t_{(9)} = -4.76, p = 0.001, \text{Cohen's } d = -1.50$ ; FDR-corrected). No significant differences between TI for untrained acute contours and 0 were observed (acute-curved contours orientated at trained orientations:  $t_{(9)} = 1.46, p = 0.209, \text{Cohen's } d = 0.46$ ; acute-straight contours orientated at trained orientations:  $t_{(9)} = 1.61, p = 0.209, \text{Cohen's } d = 0.51$ ; acute-curved contours orientated at untrained

orientations:  $t_{(9)} = 1.32, p = 0.218$ , Cohen's  $d = 0.42$ ; acute-straight contours orientated at untrained orientations:  $t_{(9)} = 1.56, p = 0.209$ , Cohen's  $d = 0.49$ ; FDR-corrected).

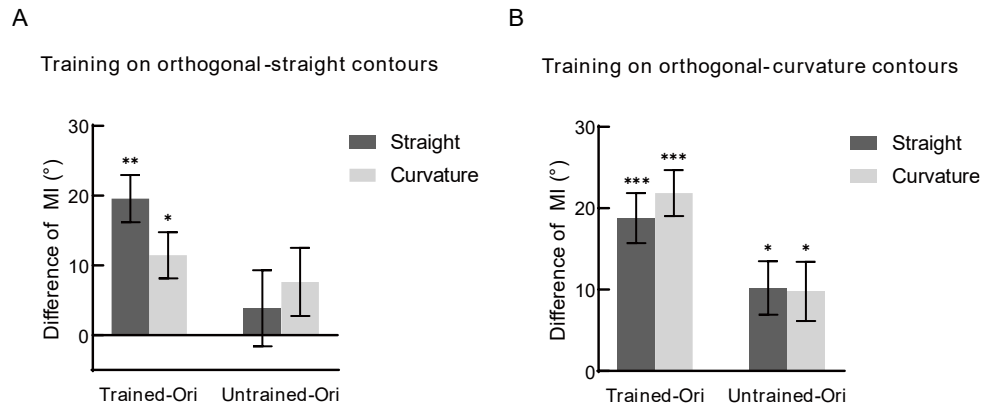


Figure 15. Difference of Performance Improvement Between Orthogonal Contours and Acute contours in Experiment 4. (A) Difference of MI in detection thresholds (Orthogonal – Acute) for trained and untrained conditions after training on orthogonal-straight contours (Experiment 4a). (B) Difference of MI in detection thresholds (Orthogonal – Acute) for trained and untrained conditions after training on orthogonal-curved contours (Experiment 4b). Asterisks indicate significant difference with 0. Error bars represent standard error of the mean across participants.

Figure. 15B shows the difference between MI for orthogonal-contour conditions and corresponding acute-contour conditions in Experiment 4b. We observed significant improvement for all four conditions (trained-path (curved)  $\times$  trained-orientation:  $t_{(9)} = 7.73, p < 0.001$ , Cohen's  $d = 2.45$ ; untrained-path (straight)  $\times$  trained-orientation:  $t_{(9)} = 6.09, p < 0.001$ , Cohen's  $d = 1.93$ ; trained-path (curved)  $\times$  untrained-orientation:  $t_{(9)} = 2.68, p = 0.025$ , Cohen's  $d = 0.85$ ; untrained-path (straight)  $\times$  untrained-orientation:  $t_{(9)} = 3.11, p = 0.017$ , Cohen's  $d = 0.98$ ; FDR-corrected). Two-way (contour path  $\times$  contour orientation) repeated-measures ANOVA revealed a significant main effect of contour orientation ( $F_{(1,9)} = 45.96, p < 0.001, \eta_p^2 = 0.84$ ). None of the other effect was significant (the main effect of contour path:  $F_{(1,9)} = 2.45, p = 0.152, \eta_p^2 = 0.21$ ; the interaction effect:  $F_{(1,9)} = 1.63, p = 0.234, \eta_p^2 = 0.15$ ).

These results indicated near-complete transfer of learning effect between contour paths, partial transfer of learning effect between contour orientations but no transfer of learning effect between contour types, supporting the learning of image regularity in stimuli during contour detection training.

No effects of training condition on the pattern of learning transfer

To compare the transfer effect of learning between Experiment 4a (training on orthogonal-straight contours) and Experiment 4b (training on orthogonal-curved contours), we performed a mixed-design ANOVA on the TI of thresholds with contour condition (seven untrained conditions) as a within-subject factor and experiment (Experiment 4a and Experiment 4b) as a between-subject factor. Neither the main effect of experiment ( $F_{(1,17)} = 0.02, p = 0.892, \eta_p^2 = 0.001$ ) nor the interaction effect ( $F_{(2,36)} = 1.07, p = 0.429, \eta_p^2 = 0.35$ ) was significant, suggesting there was no significant difference in transfer effect between the two experiments.

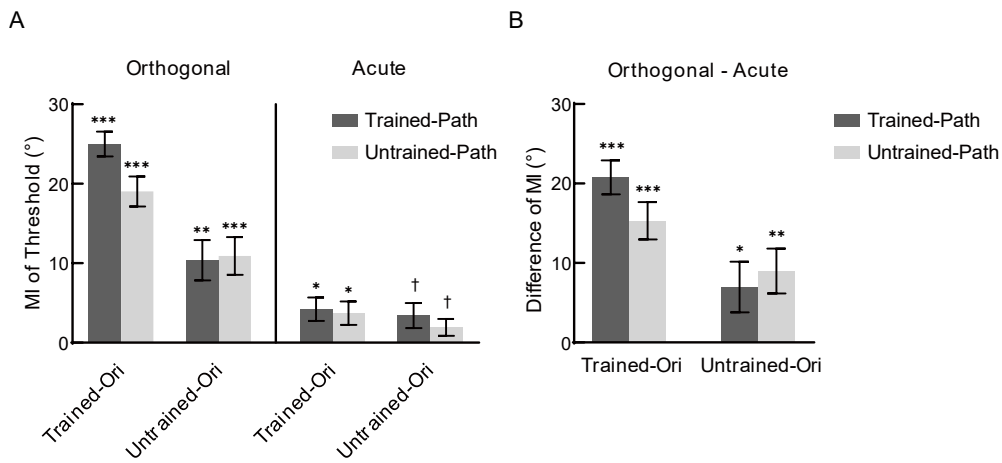


Figure 16. Performance Improvement in Experiment 4. (A) Combined MI of detection thresholds for trained and untrained conditions across Experiment 4a and Experiment 4b. (B) The combined difference between MI for orthogonal-contour conditions and that for acute-contour conditions across Experiment 4a and Experiment 4b. Asterisks indicate significant difference with 0. Error bars represent standard error of the mean across participants.

Similar to Experiment 3, a mixed-design ANOVA (experiment  $\times$  contour type  $\times$  contour path  $\times$  contour orientation) revealed no significant difference between performance improvement in Experiment 4a and Experiment 4b (experiment  $\times$  contour type  $\times$  contour path  $\times$  contour orientation:  $F_{(1,17)} = 1.72, p = 0.208, \eta_p^2 = 0.09$ ; experiment  $\times$  contour type  $\times$  contour path:  $F_{(1,17)} = 0.10, p = 0.75, \eta_p^2 = 0.006$ ; experiment  $\times$  contour type  $\times$  contour orientation:  $F_{(1,17)} = 0.01, p = 0.911, \eta_p^2 = 0.001$ ; experiment  $\times$  contour type:  $F_{(1,17)} = 1.13, p = 0.303, \eta_p^2 = 0.06$ ; experiment  $\times$  contour path:  $F_{(1,17)} = 3.43, p = 0.082, \eta_p^2 = 0.17$ ; experiment  $\times$  contour orientation:  $F_{(1,17)} = 0.33, p = 0.572, \eta_p^2 = 0.02$ ; the main effect of experiment:  $F_{(1,17)} = 0.008, p = 0.931, \eta_p^2 = 0$ ). So, we further combined

contour conditions across Experiment 4a and Experiment 4b to expand the sample amount and confirm the transfer of learning. As shown in Figure. 16A, the pooled results ( $n = 19$ ) showed significant improvements for four orthogonal-contour conditions (orthogonal  $\times$  trained-path  $\times$  trained-orientation:  $t_{(18)} = 15.94$ ,  $p < 0.001$ , Cohen's  $d = 3.66$ ; orthogonal  $\times$  untrained-path  $\times$  trained-orientation:  $t_{(18)} = 10.08$ ,  $p < 0.001$ , Cohen's  $d = 2.31$ ; orthogonal  $\times$  trained-path  $\times$  untrained-orientation:  $t_{(18)} = 4.09$ ,  $p = 0.001$ , Cohen's  $d = 0.94$ ; orthogonal  $\times$  untrained-path  $\times$  untrained-orientation:  $t_{(18)} = 4.59$ ,  $p < 0.001$ , Cohen's  $d = 1.05$ ; FDR-corrected) and two acute-contours conditions orientated at trained orientations (acute  $\times$  trained-path  $\times$  trained-orientation:  $t_{(18)} = 2.87$ ,  $p = 0.016$ , Cohen's  $d = 0.66$ ; acute  $\times$  untrained-path  $\times$  trained-orientation:  $t_{(18)} = 2.52$ ,  $p = 0.029$ , Cohen's  $d = 0.58$ ; FDR-corrected). The improvements for acute-contour condition orientated at untrained orientations were marginally significant (acute  $\times$  trained-path  $\times$  untrained-orientation:  $t_{(18)} = 2.16$ ,  $p = 0.051$ , Cohen's  $d = 0.50$ ; acute  $\times$  untrained-path  $\times$  untrained-orientation:  $t_{(18)} = 1.82$ ,  $p = 0.086$ , Cohen's  $d = 0.42$ ; FDR-corrected). Three-way (contour type  $\times$  contour path  $\times$  contour orientation) repeated-measures ANOVA revealed significant three-factor interaction ( $F_{(1,18)} = 5.28$ ,  $p = 0.034$ ,  $\eta_p^2 = 0.23$ ), and further two-way (contour path  $\times$  contour orientation) repeated-measures ANOVA on MI for orthogonal contours also revealed significant interaction effect ( $F_{(1,18)} = 8.85$ ,  $p = 0.008$ ,  $\eta_p^2 = 0.33$ ) and significant main effects of contour path ( $F_{(1,18)} = 10.89$ ,  $p = 0.004$ ,  $\eta_p^2 = 0.38$ ) and orientation ( $F_{(1,18)} = 38.12$ ,  $p < 0.001$ ,  $\eta_p^2 = 0.68$ ). Simple effect analysis showed significantly higher performance improvement for orthogonal contours with trained paths compared to orthogonal contours with untrained paths only when contours orientated at trained orientations ( $t_{(18)} = 4.46$ ,  $p < 0.001$ , Cohen's  $d = 1.02$ ), and significant higher improvement for orthogonal contours orientated at trained orientations than orthogonal contours orientated at untrained orientations no matter contour paths were trained ( $t_{(18)} = 6.24$ ,  $p < 0.001$ , Cohen's  $d = 1.43$ ) or untrained ( $t_{(18)} = 4.23$ ,  $p < 0.001$ , Cohen's  $d = 0.97$ ). Two-way (contour path  $\times$  contour orientation) repeated-measures ANOVA on MI for acute contours showed no significant effect (the main effect of path:  $F_{(1,18)} = 1.03$ ,  $p = 0.323$ ,  $\eta_p^2 = 0.05$ ; the main effect of orientation:  $F_{(1,18)} = 0.59$ ,  $p = 0.452$ ,  $\eta_p^2 = 0.03$ ; the interaction effect:  $F_{(1,18)} = 0.31$ ,  $p = 0.586$ ,  $\eta_p^2 = 0.02$ ).

We also combined the difference between MI for orthogonal-contour conditions and that for acute-contour conditions across Experiment 4a and Experiment 4b since there was no significant difference between that in the two experiments (mixed-design ANOVA; experiment  $\times$  contour path

× contour orientation:  $F_{(1,17)} = 1.72, p = 0.208, \eta_p^2 = 0.09$ ; experiment × contour path:  $F_{(1,17)} = 0.10, p = 0.753, \eta_p^2 = 0.006$ ; experiment × contour orientation:  $F_{(1,17)} = 0.01, p = 0.911, \eta_p^2 = 0.001$ ; the main effect of experiment:  $F_{(1,17)} = 1.13, p = 0.303, \eta_p^2 = 0.06$ ). As shown in Figure. 16B, one-sample t-tests on the combined difference of MI between orthogonal contours and acute contours ( $n = 19$ ) revealed significant improvement for all four conditions (trained-path × trained-orientation:  $t_{(18)} = 9.70, p < 0.001, \text{Cohen's } d = 2.23$ ; untrained-path × trained-orientation:  $t_{(18)} = 6.50, p < 0.001, \text{Cohen's } d = 1.49$ ; trained-path × untrained-orientation:  $t_{(18)} = 2.18, p = 0.043, \text{Cohen's } d = 0.50$ ; untrained-path × untrained-orientation:  $t_{(18)} = 3.19, p = 0.007, \text{Cohen's } d = 0.73$ ; FDR-corrected). Two-way (contour path × contour orientation) repeated-measures ANOVA revealed significant interaction effect ( $F_{(1,18)} = 5.28, p = 0.034, \eta_p^2 = 0.23$ ) and main effect of contour orientation ( $F_{(1,18)} = 17.69, p < 0.001, \eta_p^2 = 0.50$ ), but no significant main effect of contour path ( $F_{(1,18)} = 1.79, p = 0.198, \eta_p^2 = 0.09$ ). Further simple effect analysis showed significantly higher performance improvement for contours with trained paths compared to contours with untrained paths only when contours orientated at trained orientations ( $t_{(18)} = 3.23, p = 0.005, \text{Cohen's } d = 0.74$ ). The improvement for contours orientated at trained orientations was significantly higher than that for contours orientated at untrained orientations, regardless of whether contour paths were trained ( $t_{(18)} = 4.47, p < 0.001, \text{Cohen's } d = 1.02$ ) or not ( $t_{(18)} = 2.36, p = 0.030, \text{Cohen's } d = 0.54$ ). Consistent with our previous findings in Experiment 3, these results confirmed the transfer of contour detection learning between contour paths and between contour orientations, supporting the learning of image regularity during contour detection training.

## Discussion

Previous studies showed that the human brain could flexibly exploit image regularities and learn to integrate signals atypical of shape contours in natural scenes (orthogonal, acute alignments), but the learning effect was specific to the contour type (Schwarzkopf & Kourtzi, 2008; Schwarzkopf & Kourtzi, 2009). In this study, we examined whether the learning effect of contour integration could transfer on the other feature dimensions (i.e., contour path and contour orientation). Consistent with previous studies, we found that the learning of contour integration showed a significant contour type specificity. Specifically, the detection performance improved significantly

for trained contour type (i.e., orthogonal alignments) but not for other contours with untrained alignments (i.e., collinear and acute alignments) after training. Apart from this, we also observed, at least, partial transfers of learning between contour paths or between contour orientations for contours with trained contour type. These results support that the visual system learns to capitalize on statistical regularities in the visual inputs for contour linking during contour detection training and advance our understanding of the essence and character of the learning of contour integration and detection in cluttered scenes.

The present study confirms previous findings that short-term experience in adulthood retunes the utility of image regularities to support the perceptual integration of contours (Schwarzkopf & Kourtzi, 2008; Schwarzkopf & Kourtzi, 2009). After training, learners learned to integrate and detect contours defined by regularities (e.g., elements orthogonal to the contour path) that typically signify discontinuities rather than coherent shape contours in natural scenes. However, this learning effect did not transfer to contours defined by other discontinuity regularity (e.g., elements at an acute angle to the contour path), although orthogonal alignments and acute alignments have similar probability of occurrence in natural scenes (Sigman et al., 2001; Geisler et al., 2001). This learning specificity for contour type is consistent with the feature-specificity of perceptual learning (Ball & Sekuler, 1982; Fiorentini & Berardi, 1981; Schoups et al., 1995; Watanabe et al., 2002), and indicates that the image regularities learned by observers during training involved the orientation of local contour elements encoded by primary visual cortex.

It is interesting to note that we observed significant performance improvements for contours with trained contour type but untrained contour path, indicating a partial, sometimes complete, transfer of contour integration learning between global contour paths. The contours in our study were either straight contours or curved contours with low curvature. There was a study showing that a neuron population in monkey visual area V4, involved in the processing of shapes of intermediate complexity, selectively responded to straight or low-curvature contours (Nandy et al., 2013), which may give us some enlightenment in the learning transfer over the contour path observed in our study.

We also observe a partial transfer of learning effect between global contour orientations, which is different from the findings reported in the previous study (Zhang & Kourtzi, 2010). In the study

of Zhang and Kourtzi (2010), the stimuli in training sessions consisted of four contour lines with large spacing between contour elements, but the stimuli in test sessions only comprised two contour lines, which was different from the design in our study that stimuli in both training sessions and test sessions consisted of 4 contour paths with smaller spacing between contour elements. It is more difficult to detect contours comprising two paths than those comprising four paths and it is more difficult to detect contours with large spacing between contour elements than those with smaller element spacing. According to previous studies, the specificity and transferability of perceptual learning are influenced by the detection difficulty of the target (Ahissar & Hochstein, 1997; DeLoss et al., 2014; Talluri et al., 2015; Wang et al., 2013). Moreover, participants in our study were trained for five or seven days, which was significantly less than the number of training sessions in Zhang and Kourtzi (2010). Studies about the effects of training amount on perceptual learning showed that prolonged training led to stronger specificity (Jeter et al., 2010; Hung & Seitz, 2014; Liang et al., 2015a; Song et al., 2021). The different results of the learning transfer between global contour orientations observed in our study and previous study may due to the differences in stimuli and training amount. Some previous studies using double training or training-plus-exposure procedures had showed transfer of perceptual learning across retina locations and stimuli features (Xiao et al., 2008; Zhang et al., 2010; Wang et al., 2016; Xiong et al., 2016). However, the learning transfer between contour paths or contour orientations observed in our study may reflect a transfer mechanism which is not exactly the same as that was revealed in these studies, in which the transfer orientation or location was exposed additionally via irrelevant tasks.

Many contour integration theories have assumed that contour integration would be mediated by the long-range horizontal connections in V1 that connects neurons with similar orientation preferences (Field et al., 1993; Li, 1998; Kapadia et al., 2000; Gilbert & Wiesel, 1989). However, some evidence showed that contour integration also involves other visual areas (Altmann et al., 2003; Kourtzi et al., 2003; Kuai et al., 2017). Studies based on monkey and human data showed that neural responses related to contour in higher-level regions such as V4 and LOC are earlier than those in V1 (Chen et al., 2014; Shpaner et al., 2013; Mijović et al., 2014) and V1 responses to contour stimuli are strongly modulated by top-down feedback (Li et al. 2006, 2008; McManus et al., 2011; Chen et al., 2014; Li et al., 2019). The observed transfer between global paths or

orientations in this study may also support the engagement of higher cortical areas in contour integration and its learning (Kourtzi et al., 2005).

According to theories about visual processing, there is a distributed hierarchy processing of visual information in the human cerebral cortex (Felleman & Van Essen, 1991). Within the hierarchy structure, at the low-level, simple local features are encoded in the early visual areas, and, at a higher level, local features combine to form more complex features encoded in higher visual areas. Along the hierarchy, neurons represent more and more complex and abstract information, which may show more generalization gradually (Fukushima, 1988; Kobatake & Tanaka, 1994; Riesenhuber & Poggio, 1999; Hochstein & Ahissar, 2002). The difference in specificity and transfer of different stimuli features, observed in our study, may be related to the levels at which these features are represented in shape and contour processing. The local orientation of contour elements (i.e., contour type) is a low-level stimulus feature that is encoded primarily by V1 neurons showing orientation selectivity (Hubel & Wiesel, 1959, 1965, 1968), which may support the contour-type specificity of contour integration learning. In contrast, the global contour path and orientation are higher-level features compared with local element orientations, and their representations involve higher occipitotemporal areas responsible for global form processing, such as V3, V4, and LO (Schwarzkopf & Kourtzi, 2009; Zhang & Kourtzi, 2010; Kuai et al. 2017). Kuai et al. (2017) reported that IPS and LO activation patterns could not discriminate the orientation of contours, implying that these higher cortical regions may be parts of the neural substrate supporting the transfer of contour integration learning observed in our study.

In sum, our findings reveal that contour integration learning shows no transfer over contour type but partial transfer over global contour path or orientation, supporting that short-term training improved the ability to integrate specific types of contours by optimizing the ability of the visual system to use specific image regularities. The different specificity and transferability over different stimulus feature dimensions provide more insights into understanding the nature of contour integration learning and indicate the involvement of both low-level and higher-level visual regions in such progress (Kourtzi et al., 2005). The precise brain plasticity mechanisms that mediate the various transfer effect of contour integration learning should be investigated in future work.

## Acknowledgment

This work was supported by the National Science and Technology Innovation 2030 Major Project Program (2022ZD0208200) and National Natural Science Foundation of China (NO. 31800910).

## References

- Ahissar, M., & Hochstein, S. (1997). Task difficulty and the specificity of perceptual learning. *Nature*, 387(6631), 401–406. <https://doi.org/10.1038/387401a0>
- Altmann, C. F., Bühlhoff, H. H., & Kourtzi, Z. (2003). Perceptual Organization of Local Elements into Global Shapes in the Human Visual Cortex. *Current Biology*, 13(4), 342–349. <https://doi.org/10/cwf73s>
- Ball, K., & Sekuler, R. (1982). A specific and enduring improvement in visual motion discrimination. *Science*, 218(4573), 697–698. <https://doi.org/10.1126/science.7134968>
- Ball, K., & Sekuler, R. (1987). Direction-specific improvement in motion discrimination. *Vision Research*, 27(6), 953–965. [https://doi.org/10.1016/0042-6989\(87\)90011-3](https://doi.org/10.1016/0042-6989(87)90011-3)
- Bex, P. J., Simmers, A. J., & Dakin, S. C. (2001). Snakes and ladders: The role of temporal modulation in visual contour integration. *Vision Research*, 41(27), 3775–3782. <https://doi.org/10/fh6g5b>
- Brainard, D. H. (1997). The Psychophysics Toolbox. *Spatial Vision*, 10(4), 433–436. <https://doi.org/10.1163/156856897X00357>
- Chen, M., Yan, Y., Gong, X., Gilbert, C. D., Liang, H., & Li, W. (2014). Incremental Integration of Global Contours through Interplay between Visual Cortical Areas. *Neuron*, 82(3), 682–694. <https://doi.org/10.1016/j.neuron.2014.03.023>

- DeLoss, D. J., Watanabe, T., & Andersen, G. J. (2014). Optimization of perceptual learning: Effects of task difficulty and external noise in older adults. *Vision Research*, *99*, 37–45. <https://doi.org/10.1016/j.visres.2013.11.003>
- Demeyer, M., & Machilsen, B. (2012). The construction of perceptual grouping displays using GERT. *Behavior Research Methods*, *44*(2), 439–446. <https://doi.org/10.3758/s13428-011-0167-8>
- Felleman, D. J., & Van Essen, D. C. (1991). Distributed Hierarchical Processing in the Primate Cerebral Cortex. *Cerebral Cortex*, *1*(1), 1–47. <https://doi.org/10.1093/cercor/1.1.1-a>
- Field, D. J., Hayes, A., & Hess, R. F. (1993). Contour integration by the human visual system: Evidence for a local “association field”. *Vision Research*, *33*(2), 173–193. <https://doi.org/10/ftfw9n>
- Fiorentini, A., & Berardi, N. (1981). Learning in grating waveform discrimination: Specificity for orientation and spatial frequency. *Vision Research*, *21*(7), 1149–1158. [https://doi.org/10.1016/0042-6989\(81\)90017-1](https://doi.org/10.1016/0042-6989(81)90017-1)
- Fukushima, K. (1988). A neural network for visual pattern recognition. *Computer*, *21*(3), 65–75. <https://doi.org/10.1109/2.32>
- Geisler, W. S., Perry, J. S., Super, B. J., & Gallogly, D. P. (2001). Edge co-occurrence in natural images predicts contour grouping performance. *Vision Research*, *41*(6), 711–724. [https://doi.org/10.1016/S0042-6989\(00\)00277-7](https://doi.org/10.1016/S0042-6989(00)00277-7)
- Geisler, W. (2008). Visual Perception and the Statistical Properties of Natural Scenes. *Annual review of psychology*, *59*, 167–192. <https://doi.org/10.1146/annurev.psych.58.110405.085632>
- Gilbert, C., & Wiesel, T. (1989). Columnar specificity of intrinsic horizontal and corticocortical connections in cat visual cortex. *The Journal of Neuroscience*, *9*(7), 2432–2442. <https://doi.org/10.1523/JNEUROSCI.09-07-02432.1989>
- Hess, R., & Field, D. (1999). Integration of contours: New insights. *Trends in Cognitive Sciences*, *3*(12), 480–486. [https://doi.org/10.1016/S1364-6613\(99\)01410-2](https://doi.org/10.1016/S1364-6613(99)01410-2)

- Hochstein, S., & Ahissar, M. (2002). View from the top: Hierarchies and reverse hierarchies in the visual system. *Neuron*, 36(5), 791–804. [https://doi.org/10.1016/s0896-6273\(02\)01091-7](https://doi.org/10.1016/s0896-6273(02)01091-7)
- Hubel, D. H., & Wiesel, T. N. (1959). Receptive fields of single neurons in the cat's striate cortex. *The Journal of Physiology*, 148, 574–591. <https://doi.org/10.1113/jphysiol.1959.sp006308>
- Hubel, D. H., & Wiesel, T. N. (1965). Receptive fields and functional architecture in two nonstriate visual areas (18 and 19) of the cat. *Journal of Neurophysiology*, 28, 229–289. <https://doi.org/10.1152/jn.1965.28.2.229>
- Hubel, D. H., & Wiesel, T. N. (1968). Receptive fields and functional architecture of monkey striate cortex. *The Journal of Physiology*, 195(1), 215–243. <https://doi.org/10.1113/jphysiol.1968.sp008455>
- Hung, S.-C., & Seitz, A. R. (2014). Prolonged Training at Threshold Promotes Robust Retinotopic Specificity in Perceptual Learning. *Journal of Neuroscience*, 34(25), 8423–8431. <https://doi.org/10.1523/JNEUROSCI.0745-14.2014>
- Jeter, P. E., Doshier, B. A., Liu, S.-H., & Lu, Z. L. (2010). Specificity of perceptual learning increases with increased training. *Vision Research*, 50, 1928–1940. <https://doi.org/10.1016/j.visres.2010.06.016>
- Kapadia, M. K., Westheimer, G., & Gilbert, C. D. (2000). Spatial Distribution of Contextual Interactions in Primary Visual Cortex and in Visual Perception. *Journal of Neurophysiology*, 84(4), 2048–2062. <https://doi.org/10/ggh3pk>
- Kleiner, M., Brainard, D.H., & Pelli, D. (2007). What's new in Psychtoolbox-3? *Perception*, 36, 1–16.
- Kobatake, E., & Tanaka, K. (1994). Neuronal selectivities to complex object features in the ventral visual pathway of the macaque cerebral cortex. *Journal of Neurophysiology*, 71(3), 856–867. <https://doi.org/10.1152/jn.1994.71.3.856>

- Kourtzi, Z., Betts, L. R., Sarkheil, P., & Welchman, A. E. (2005). Distributed neural plasticity for shape learning in the human visual cortex. *PLoS Biology*, 3(7), e204. <https://doi.org/10.1371/journal.pbio.0030204>
- Kourtzi, Z., Tolias, A. S., Altmann, C. F., Augath, M., & Logothetis, N. K. (2003). Integration of Local Features into Global Shapes: Monkey and Human fMRI Studies. *Neuron*, 37(2), 333–346. [https://doi.org/10.1016/S0896-6273\(02\)01174-1](https://doi.org/10.1016/S0896-6273(02)01174-1)
- Kuai, S.-G., Li, W., Yu, C., & Kourtzi, Z. (2016). Contour Integration over Time: Psychophysical and fMRI Evidence. *Cerebral Cortex*, bhw147. <https://doi.org/10.1093/cercor/bhw147>
- Ledgeway, T., Hess, R. F., & Geisler, W. S. (2005). Grouping local orientation and direction signals to extract spatial contours: Empirical tests of “association field” models of contour integration. *Vision Research*, 45(19), 2511–2522. <https://doi.org/10/bfdhd8>
- Li, W., Piëch, V., & Gilbert, C. D. (2006). Contour Saliency in Primary Visual Cortex. *Neuron*, 50(6), 951–962. <https://doi.org/10.1016/j.neuron.2006.04.035>
- Li, W., Piëch, V., & Gilbert, C. D. (2008). Learning to Link Visual Contours. *Neuron*, 57(3), 442–451. <https://doi.org/10.1016/j.neuron.2007.12.011>
- Li, Y., Wang, Y., & Li, S. (2019). Recurrent Processing of Contour Integration in the Human Visual Cortex as Revealed By fMRI-Guided TMS. *Cerebral Cortex (New York, N.Y.)*, 29(1), 17–26. <https://doi.org/10/gck3x2>
- Li, Z. (1998). A neural model of contour integration in the primary visual cortex. *Neural Computation*, 10(4), 903–940. <https://doi.org/10/dmcfxr>
- Liang, J., Zhou, Y., Fahle, M., & Liu, Z. (2015). Limited transfer of long-term motion perceptual learning with double training. *Journal of Vision*, 15(10), 1. <https://doi.org/10.1167/15.10.1>

- Liu, Z. (1999). Perceptual learning in motion discrimination that generalizes across motion directions. *Proceedings of the National Academy of Sciences*, 96(24), 14085–14087. <https://doi.org/10.1073/pnas.96.24.14085>
- McManus, J. N. J., Li, W., & Gilbert, C. D. (2011). Adaptive shape processing in primary visual cortex. *Proceedings of the National Academy of Sciences of the United States of America*, 108(24), 9739–9746. <https://doi.org/10.1073/pnas.1105855108>
- Mijović, B., De Vos, M., Vanderperren, K., Machilsen, B., Sunaert, S., Van Huffel, S., & Wagemans, J. (2014). The dynamics of contour integration: A simultaneous EEG–fMRI study. *NeuroImage*, 88, 10–21. <https://doi.org/10.1016/j.neuroimage.2013.11.032>
- Nandy, A. S., Sharpee, T. O., Reynolds, J. H., & Mitchell, J. F. (2013). The Fine Structure of Shape Tuning in Area V4. *Neuron*, 78(6), 1102–1115. <https://doi.org/10.1016/j.neuron.2013.04.016>
- Riesenhuber, M., & Poggio, T. (1999). Hierarchical models of object recognition in cortex. *Nature Neuroscience*, 2(11), 1019–1025. <https://doi.org/10.1038/14819>
- Schoups, A. A., Vogels, R., & Orban, G. A. (1995). Human perceptual learning in identifying the oblique orientation: Retinotopy, orientation specificity and monocularly. *The Journal of Physiology*, 483(3), 797–810. <https://doi.org/10.1113/jphysiol.1995.sp020623>
- Schwarzkoepf, D. S., & Kourtzi, Z. (2008). Experience Shapes the Utility of Natural Statistics for Perceptual Contour Integration. *Current Biology*, 18(15), 1162–1167. <https://doi.org/10.1016/j.cub.2008.06.072>
- Schwarzkoepf, D. S., Zhang, J., & Kourtzi, Z. (2009). Flexible Learning of Natural Statistics in the Human Brain. *Journal of Neurophysiology*, 102(3), 1854–1867. <https://doi.org/10.1152/jn.0094>
- Shpaner, M., Molholm, S., Forde, E., & Foxe, J. J. (2013). Disambiguating the roles of area V1 and the lateral occipital complex (LOC) in contour integration. *NeuroImage*, 69, 146–156. <https://doi.org/10.1016/j.neuroimage.2012.11.023>

- Sigman, M., Cecchi, G. A., Gilbert, C. D., & Magnasco, M. O. (2001). On a common circle: Natural scenes and Gestalt rules. *Proceedings of the National Academy of Sciences of the United States of America*, 98(4), 1935–1940. <https://www.ncbi.nlm.nih.gov/pmc/articles/PMC29360/>
- Simoncelli, E., & Olshausen, B. (2001). Natural Image Statistics and Neural Representation. *Annual review of neuroscience*, 24, 1193–1216. <https://doi.org/10.1146/annurev.neuro.24.1.1193>
- Song, Y., Chen, N., & Fang, F. (2021). Effects of daily training amount on visual motion perceptual learning. *Journal of Vision*, 21(4), 6. <https://doi.org/10.1167/jov.21.4.6>
- Talluri, B. C., Hung, S.-C., Seitz, A. R., & Seriès, P. (2015). Confidence-based integrated reweighting model of task-difficulty explains location-based specificity in perceptual learning. *Journal of Vision*, 15(10), 1-12. <https://doi.org/10.1167/15.10.17>
- Tan, Q., Wang, Z., Sasaki, Y., & Watanabe, T. (2019). Category-Induced Transfer of Visual Perceptual Learning. *Current Biology*, 29(8), 1374-1378.e3. <https://doi.org/10/gfxmwp>
- Vancleef, K., & Wagemans, J. (2013). Component processes in contour integration: A direct comparison between snakes and ladders in a detection and a shape discrimination task. *Vision Research*, 92, 39–46. <https://doi.org/10/f5fqgz>
- Wang, X., Zhou, Y., & Liu, Z. (2013). Transfer in motion perceptual learning depends on the difficulty of the training task. *Journal of Vision*, 13(7), 1-9. <https://doi.org/10.1167/13.7.5>
- Wang, R., Wang, J., Zhang, J.-Y., Xie, X.-Y., Yang, Y.-X., Luo, S.-H., Yu, C., & Li, W. (2016). Perceptual Learning at a Conceptual Level. *Journal of Neuroscience*, 36(7), 2238–2246. <https://doi.org/10/f8bqfs>
- Watanabe, T., Náñez, J. E., Koyama, S., Mukai, I., Liederman, J., & Sasaki, Y. (2002). Greater plasticity in lower-level than higher-level visual motion processing in a passive perceptual learning task. *Nature Neuroscience*, 5(10), 1003–1009. <https://doi.org/10.1038/nn915>

- Xiao, L.-Q., Zhang, J.-Y., Wang, R., Klein, S. A., Levi, D. M., & Yu, C. (2008). Complete Transfer of Perceptual Learning across Retinal Locations Enabled by Double Training. *Current Biology*, *18*(24), 1922–1926. <https://doi.org/10/fkgf72>
- Xiong, Y.-Z., Zhang, J.-Y., & Yu, C. (2016). Bottom-up and top-down influences at untrained conditions determine perceptual learning specificity and transfer. *eLife*, *5*, e14614. <https://doi.org/10.7554/eLife.14614>
- Yu, C., Klein, S. A., & Levi, D. M. (2004). Perceptual learning in contrast discrimination and the (minimal) role of context. *Journal of Vision*, *4*(3), 169–182. <https://doi.org/10.1167/4.3.4>
- Zhang, J., & Kourtzi, Z. (2010). Learning-dependent plasticity with and without training in the human brain. *Proceedings of the National Academy of Sciences*, *107*(30), 13503–13508. <https://doi.org/10.1073/pnas.1002506107>
- Zhang, J. Y., & Yang, Y. X. (2014). Perceptual learning of motion direction discrimination transfers to an opposite direction with TPE training. *Vision Research*, *99*(6), 93–98. <https://doi.org/10/f55vtf>